Moldable plastics (polycaprolactone) can be acutely toxic to developing zebrafish and activate nuclear receptors in mammalian cells

Bryan D. James,[1,2,*] Alexander V. Medvedev,[3] Sergei S. Makarov,[3] Robert K. Nelson,[1] Christopher M. Reddy,[1] Mark E. Hahn[2]

[1]Department of Marine Chemistry and Geochemistry, Woods Hole Oceanographic Institution, Woods Hole, MA, USA 02543

[2]Department of Biology, Woods Hole Oceanographic Institution, Woods Hole, MA, USA 02543

[3]Attagene, Research Triangle Park, Morrisville, NC, USA 27709

*Corresponding author; Email: bjames@whoi.edu

Abstract

Popularized on social media, hand-moldable plastics are formed by consumers into tools, trinkets, and dental prosthetics. Despite the anticipated dermal and oral contact, manufacturers share little information with consumers about these materials, which are typically sold as microplastic-sized resin pellets. Inherent to their function, moldable plastics pose a risk of dermal and oral exposure to unknown leachable substances. We analyzed 12 moldable plastics advertised for modeling and dental applications and determined them to be polycaprolactone (PCL) or thermoplastic polyurethane (TPU). The bioactivities of the most popular brands advertised for modeling applications of each type of polymer were evaluated using a zebrafish embryo bioassay. While water-borne exposure to the TPU pellets did not affect the targeted developmental endpoints at any concentration tested, the PCL pellets were acutely toxic above 1 pellet/mL. Aqueous leachates of the PCL pellets demonstrated similar toxicity. Methanolic extracts from the PCL pellets were assayed for their bioactivity using the Attagene FACTORIAL platform. Of the 69 measured endpoints, the extracts activated nuclear receptors and transcription factors for xenobiotic metabolism (pregnane X receptor, PXR), lipid metabolism (peroxisome proliferator-activated receptor γ, PPARγ), and oxidative stress (nuclear factor erythroid 2-related factor 2, NRF2). By non-targeted high-resolution comprehensive two-dimensional gas chromatography (GC×GC-HRT), we tentatively identified several compounds in the methanolic extracts, including PCL oligomers, a phenolic antioxidant, and residues of suspected anti-hydrolysis and crosslinking additives. In a follow-up zebrafish embryo bioassay, because of its stated high purity, biomedical grade PCL was tested to mitigate any confounding effects due to chemical additives in the PCL pellets; it elicited comparable acute toxicity. From these orthogonal and complementary experiments, we suggest that the toxicity was due to oligomers and nanoplastics released from the PCL rather than chemical additives. These results challenge the perceived and assumed inertness of plastics and highlight their multiple sources of toxicity.

Keywords: *nanoplastics, oligomers, polyesters, polymer biocompatibility, erodible polymers*

INTRODUCTION

Evidence shows that everyday consumer plastic products leach and expose us to bioactive compounds,[1–6] of which for many their bioactivity is unknown.[7] These exposures can result from volatilized chemicals (e.g., new car smell[8]), migration of chemicals into the foods and beverages we consume,[9] and inhalation of household dust,[10] among other routes. The transport of the plastic-associated chemicals–and thus exposure to them–is accelerated when plastics are heated (e.g., microwaving food stored in plastic containers[11]). Exposures to plastic-associated chemicals have had substantial impacts on human health. The U.S. health burden of only three classes (phthalates, bisphenols, and brominated flame retardants) of the tens of thousands of chemicals used in plastics has been estimated to cost more than $600 billion annually.[4]

These facts raise concern for consumers using moldable plastics, products that frequently trend on social media because of their versatility for making artistic and practical items. Moldable plastics are pelletized plastics (~3 mm in diameter; microplastic-sized) with relatively low melting temperatures (~60 ºC) advertised as durable and usable modeling materials. Consumers are instructed to melt the pellets by heating them in boiling water for several minutes and then mold the plastic by hand, presenting an inherent opportunity for exposure to any chemicals contained within the plastic. While these materials are marketed as non-toxic, little information about them is communicated to consumers. This uncertainty has led consumers to query online forums, such as Physics Forum,[12] and product pages for answers, asking whether using these materials pose any risk, to which they have received little definitive guidance from other users and vendors.

Moreover, due to their white color, moldable plastics have been patented[13] and marketed to consumers for fashioning or securing false or prosthetic teeth (e.g., Instant Smile[14]). Such use implies short- and potentially long-term oral exposure from something purchased for a positive

outcome. Dentists have urged consumers not to use moldable plastics in this way primarily because of potential choking hazards.[15,16] To our knowledge, these products are neither cleared nor listed as medical devices by the United States Food and Drug Administration (FDA).[17]

Hence, we became curious about the potential toxicity of moldable plastics, especially because the plastics' molding process leads to dermal and oral exposure with the potential for increased risk for additives to leach and migrate when exposed to elevated temperatures. To receive a positive FDA evaluation, medical devices must demonstrate that any extractable and leachable compounds are biocompatible and not cytotoxic (e.g., ISO 10993-1). Given that moldable plastics are marketed as non-toxic and perceived to be safe by vendors and consumers, it is prudent to determine their bioactivity (if any), as well as the potential for intentionally or unintentionally added substances to leach from the material.

Evaluating the bioactivity of plastic-associated chemicals has been approached by a combination of chemical analyses, *in vitro* reporter bioassays, and *in vivo* toxicity assessments. High-resolution mass spectrometry of plastic solvent-extracts are routine assessments for food-contact and biomedical device materials.[18] Owing to the tens of thousands of potential added and non-intentionally added chemicals found in plastics and the limited disclosure of plastic formulations,[19] non-targeted analyses have become the de facto approach to understanding the complex mixture of plastic-associated chemicals in consumer products.[5] Reporter bioassays for specific nuclear receptors and biological endpoints have been used to screen extracts and leachates from consumer plastics, revealing that plastic-associated chemicals in consumer products have the potential to disrupt endocrine and metabolic processes.[1–3,5] Though targeted bioassays have been valuable, high-throughput, non-targeted screens of 50+ endpoints using the Attagene FACTORIAL platform can provide a greater depth of bioactivity, capable of assigning chemicals and complex mixtures to specific modes of action.[20–22] Complementing *in vitro* reporter assays, *in*

vivo bioassays with model organisms can elucidate the effects of chemical exposures on development and behavior. Zebrafish are a widely used model organism in chemical and material toxicology because of their rapid development, ease of use, and well-documented phenotypes and responses to chemical toxicants (e.g., polycyclic aromatic hydrocarbons, polychlorinated biphenyls, and bisphenol A).[23,24] Additionally, fish embryos can be more susceptible to toxicants during early development, thus providing greater sensitivity to the effects of any leached chemicals from the moldable plastic. Exposure to plastics and their associated chemicals has often resulted in sublethal effects reflected by changes in gene expression, metabolic activity, and behavior.[25–28] Only in a few instances have plastic items been acutely toxic to zebrafish embryos. In these cases, toxicity has been attributed to the release of a residual non-intentionally added substance (e.g., acrylate monomer or surfactant).[29,30]

Herein, we purchased commercially available moldable plastic products and evaluated the toxicity of the two most popular brands using a zebrafish developmental bioassay, assessed the bioactivity of their methanolic extracts using the advanced Attagene FACTORIAL platform, and characterized the extracts by high-resolution comprehensive two-dimensional gas chromatography (GC×GC-HRT). Our results indicated that some products exhibit acute toxicity and bioactivity that originated from a mixture of degradation and residual oligomers of the plastic (and less likely chemical additives), conflicting with the presumed biological inertness of these polymers by vendors and consumers.

MATERIALS AND METHODS

Materials included in a survey of moldable plastics on the market

All moldable plastic products were purchased on Amazon.com. Products were selected by searching with combinations of "PCL", "moldable", "dental", "teeth", and "pellet". These terms yielded ~500 results, many of which were redundant. Twelve different products were chosen to reflect a range of customer ratings, number of reviews and ratings, and various forms (e.g., pellets, sheets, and filaments) (**Table 1**).

Moldable plastics advertised for general purpose included,

- "InstaMorph | Thermoplastic Beads, Meltable Polymorph Pellets | Lightweight Modeling Compound for DIY Crafts, Sculpting, Cosplay Accessories | Temporarily Repair | Six Ounce White" sold by Instamorph,
- “Moldable Plastic Thermoplastic Beads 8OZ, White” sold by JXE JXO,
- "Polly Plastics Heat Moldable Plastic Sheets" sold by Polly Plastics,
- "50g Thermoplastic Models Moldable Low-Melting Polycaprolactone PCL Crystalline Hydrophobic Polyester Polymers Plastic Beads Pellets" sold by PeakCargo HK and branded as Perstorp CAPA 6800 grade PCL on the packaging, and
- "uxcell 3D Pen Filament Refills,16Ft,1.75mm PCL Filament Refills, Dimensional Accuracy +/- 0.02mm, for 3D Printer, White" sold by uxcell.

Moldable plastics advertised for use as oral prosthetics included,

- "Rubie's Costume Co Teeth Pellets" sold by Rubie's,
- “Fitting Beads, 3 Pack Included, Can Be Used for Any Billy Bob Teeth OR Instant Smile Teeth!”, sold by Billy Bob,
- "Imako Cosmetic Teeth Extras (Pink and White Fitting Material)" sold by Imako, "SmileFix Basic Dental Repair Kit - Missing or Broken Tooth. Gaps, Broken Teeth Filled Space

Temporary Quick & Safe. Regain Your Confidence and Beautiful Smile in Minutes at Home!" sold by Smile Fix,

- "JJ CARE Temporary Tooth Replacement Kit with Dental Tools, Moldable Thermoplastic Beads Tooth Filler for Gaps, Missing or Broken Tooth, DIY Chipped Tooth Repair Kit for up to 20 Teeth Repair" sold by JJ Care,
- "Brige Temporary Tooth Repair kit for Filling The Missing Broken Tooth and Gaps-Moldable Fake Teeth and Thermal Beads Replacement Kit" sold by Brige, and
- "Temporary Tooth Repair Kits, Dental Repair Denture Repair Beads, Tweezers, Dental Pick, Dental Tools for Temporary Fixing Filling Missing Broken Tooth Moldable Fake Teeth" sold by Waxxy and labeled as J Moldable.

Biomedical-grade polycaprolactone (PCL) (Purasorb PC17; GMP grade homopolymer) was purchased from Sigma Aldrich (Product Number: 900820, Batch Number: MKCN6057). Each plastic was stored at room temperature under ambient conditions.

Polymer identification by attenuated total reflectance-Fourier transform infrared spectroscopy (ATR-FTIR)

An IR spectrum of each moldable plastic product was collected using an Agilent Cary 630 FTIR with a diamond crystal ATR module, with an average of 32 scans with 2 cm^{-1} resolution. Spectra were processed in Open Specy,[31] applying a linear baseline and first-order smoothing, and assigned polymer identity (Pearson's $r > 0.95$) based on comparison to the Open Specy database of ~600 spectra, consisting of a range of polymers and materials. Pearson's r statistic was calculated automatically in Open Specy.

Bulk elemental analysis

The bulk elemental carbon, hydrogen, and nitrogen content of the moldable plastic products (samples of 15 mg or more) was measured by Midwest Microlabs (Indianapolis, IN, USA) (**Table 1**). The reported accuracy was ~0.3%, with a minimal detection limit of 0.15% for each element.[32,33]

Morphometric and colorimetric analysis

Individual moldable plastic pellets were illuminated on a tracing board and imaged using a Celestron digital microscope (Product #44308). Images were processed with the National Institutes of Health (NIH) ImageJ (1.53f51) software using the methods of James et al.[34] previously applied to analyzing images of polyethylene pellets. Several image-based metrics were determined, including the pellet's perimeter, area, circularity, aspect ratio, hue, saturation, and brightness.

Animal husbandry

Adult wild-type AB strain zebrafish (*Danio rerio*) were housed in 10 L tanks in a fish-rearing system (Iwaki Aquatic Systems, Holliston, MA, USA). The fish were held in approximately 2:1 female to male cohorts at a density of 3-4 fish/L in buffered freshwater (475.5 mg/L Instant Ocean, 79.3 mg/L $NaHCO_3$, and 53.8 mg/L $CaSO_4$, pH 7.2.-7.5). The photoperiod was set to a 14:10 h light:dark cycle, and the water temperature was kept at 28.5 °C. The fish were fed twice daily, consisting of live brine shrimp (*Artemia salina*) in the morning and GEMMA Micro 300 micro-pellets (Skretting) in the afternoon. Freshly fertilized eggs were obtained by breeding multiple tanks. Viable embryos were collected, pooled, and maintained at 28-28.5 °C with a 14:10 light-dark cycle in egg water (60 µg/mL Instant Ocean) with a drop of methylene blue. The Woods Hole

Oceanographic Institution Animal Care and Use Committee (Assurance D16-00381 from the NIH Office of Laboratory Animal Welfare) approved all experiments.

Static developmental bioassays

The toxicity of the plastics and their leachates were tested using three different configurations of a zebrafish developmental bioassay. For configuration one, embryos were continuously exposed to each plastic starting at ~4 h post-fertilization (hpf) until three days post-fertilization (dpf), unless otherwise noted, in freshly made, sterile filtered (0.2 μm pore size) 10% Hank's embryo medium[35] (10.37 mM NaCl, 0.54 mM KCl, 0.025 mM Na_2HPO_4, 0.044 mM KH_2PO_4, 0.13 mM $CaCl_2$, 0.1 mM $MgSO_4$, 0.42 mM $NaHCO_3$, pH 7.2). Treatments included Instamorph and JXE JXO pellets, as well as biomedical-grade PCL. Embryos were evaluated daily for mortality. For configuration two, embryos were continuously exposed to 4 Instamorph pellets/mL starting at ~4, 24, and 48 hpf in freshly made, sterile filtered 10% Hank's embryo medium. After 24 h of exposure, embryos were assessed for mortality. The time points for starting exposure were selected because they correspond to different stages of zebrafish embryo development, 4 hpf being the segmentation period, 24 hpf being the pharyngula period, and 48 hpf being the hatching period. For configuration three, embryos were continuously exposed to leachates prepared from Instamorph pellets or pre-leached Instamorph pellets starting at ~4 hpf in freshly made, sterile filtered 10% Hank's embryo medium. Leachates were prepared immediately before the exposure experiment by leaching Instamorph pellets for 24 h at room temperature in freshly made, sterile filtered 10% Hanks embryo medium with 4 pellets/mL. After leaching, the pellets were collected and used as pre-leached pellets. Embryos were evaluated daily for mortality. In all configurations, viable AB strain zebrafish embryos were used, untreated embryos were used as a control treatment, and each replicate had ten embryos in 5 mL of medium maintained in 60 mm diameter combusted borosilicate glass Petri dishes at 28 ± 0.5°C.

Solvent extracts

Three different solvent extracts were prepared by incubating three sets of 10 Instamorph pellets in 5 mL analytical grade methanol (~30 mg/mL) for 24 h at room temperature in combusted borosilicate glass vials with PTFE/F217 lined caps. Methanol was chosen because it can extract polar compounds[1–3,5] without dissolving PCL. After extraction, half of the extracts (2.5 mL) were evaporated under a gentle stream of nitrogen at room temperature and reconstituted in 100 µL of molecular biology grade dimethyl sulfoxide (DMSO) for high-throughput screening bioassays. Additionally, 1.5 mL of an extract was exposed to a gentle stream of nitrogen at room temperature until dryness and reconstituted in 100 µL analytical grade dichloromethane (DCM) for non-targeted analyses by GC×GC. An extraction blank without plastic was also prepared for the bioassays and the GC analyses. Specifics of each extract are provided in **Table S1**.

High-throughput screening bioassays

DMSO-reconstituted methanolic extracts were shipped to Attagene, Inc. (Morrisville, NC, USA) for testing by their TF-FACTORIAL (45 TF specific reporters) and NR-FACTORIAL (24 human NRs) assays (previously named cis- and trans- FACTORIAL assays, respectively).[21,22] The assays use HepG2 cells to assess the activity of endogenous transcription factors (TF) or transfected hybrid proteins consisting of a yeast GAL4 DNA binding domain and ligand-binding domain of the human nuclear receptors (NR). These multiplexed assays comprised 69 measured endpoints (**Table S2**) related to cell stress, endocrine activity, growth and differentiation, immunity, and lipid, xenobiotic, and general metabolism. Extracts were tested at a single concentration (3 µL DMSO extract/mL cell culture medium) for 24 h for the NR-FACTORIAL assay and at three concentrations (1, 3, and 9 µL DMSO extract/mL cell culture medium) for 24 h for the

TF-FACTORIAL assay. The TF-FACTORIAL assay was repeated twice at the midpoint concentration. Final DMSO concentrations were 0.1-0.9% (v/v), depending on the concentration of extract used in the assay. Three to six technical replicates of DMSO solvent controls matched to the DMSO concentration of the extracts were run with each sample set. Each extract was run as three technical replicates in Dulbecco's Modified Eagle Medium (DMEM) containing 1% charcoal-stripped fetal bovine serum (FBS). Reporter RNA was isolated, amplified by reverse-transcription polymerase chain reaction (RT-PCR), labeled with fluorescent markers, and quantitively assayed by capillary electrophoresis. Bioassay responses were expressed as fold-induction relative to the DMSO control by dividing the treated cells' average technical replicate expression by the average technical replicate expression of the appropriate DMSO control. Additional details of the bioassays are provided in Blackwell et al.[36]

Non-targeted comprehensive two-dimensional gas chromatography (GC×GC)

Because the three methanolic extracts were each prepared from a random composite of 10 pellets of the same material (Instamorph pellets), as a representative sample, only one DCM-reconstituted methanolic extract (sample one, **Table S1**) was analyzed by GC×GC. The extraction blank was analyzed as well. Samples were analyzed by GC×GC-FID and GC×GC-HRT using published methods[32,37–40] routine to the Organic Geochemistry Analysis Laboratory - GC×GC Facility at the Woods Hole Oceanographic Institution. Chromatographic peaks were tentatively identified based on mass spectral matches (above 80% similarity; NIST/EPA/NIH 20 Mass Spectral Library) and mass spectral interpretation.[39] See the **Supporting Information** for complete methods.

Statistical analysis

Statistical analyses were conducted using GraphPad Prism 10.1.0 (264). Data are presented as the mean ± standard deviation (n = replication). Groups were considered significantly different for a *p* value less than 0.05. Sample sizes and statistical tests are included in the text and figure captions where appropriate. Data evaluated by ANOVA satisfied normality and variance assumptions as determined by the D'Agostino-Pearson omnibus test for normality of the residuals and the Brown-Forsythe test for homoscedasticity.

RESULTS

The information made readily available by retailers of moldable plastics was scant and non-specific

We purchased 12 moldable plastics from Amazon.com that were advertised for modeling and dental applications and reflected a range of user ratings (**Table 1**). We reviewed each plastic's product page on Amazon.com and the vendor website (if applicable) for details about the plastic used for each product. Descriptions and information on the polymers were limited. Many of the plastics were described in vague and generic terms such as "polyester", "white beads", "thermoplastic polymer", "shapeable resin", and "thermoplastic beads".

Many of the products sold for dental applications included a legal disclaimer on their Amazon.com webpage stating their lack of FDA evaluation. These products can be considered as either "temporary crown and bridge resin" or "tooth shade resin material",[41,42] making them class II medical devices. Thus, they are regulated by the FDA via the 510(k) pathway, requiring premarket notification to "clear" the product before commercial distribution. None of the analyzed moldable plastics were listed in the FDA 510(k) premarket notification database (**Tables S3-S4**) or in any

other FDA database as approved, cleared, or authorized medical devices.[43,44] It should be noted that the FDA only approves medical devices, not their materials, i.e., using a material that is part of one approved medical device does not indicate that the material is safe for use in another application.

Only a few products had readily available safety data sheets (SDS) accessible to download on the product page or vendor's website. None of the plastics advertised for dental applications had SDSs. According to the few available SDSs, the materials were PCL.[45–48] Additionally, PCL is listed as the preferred embodiment material in the patent describing the use of moldable plastics to fashion dental prosthetics.[13] Therefore, we initially assumed that all moldable plastics on the market were PCL. According to reviews, customers also believed that these materials were PCL. However, they noted differences between products. For instance, one reviewer stated that, when melted, JXE JXO plastic was "stickier" than Instamorph plastic,[49] suggesting that it might be a different polymer.

Consumer-grade moldable plastics were polycaprolactone (PCL) or thermoplastic polyurethane (TPU)

The moldable plastics ranged in shape and color. Most moldable plastic products were ellipsoid resin pellets (**Figure 1A**). Visually, the pellets were indistinguishable from product to product (**Figure 1A**). One product was a thick sheet (Polly Plastic), and another was a filament (uxcell). All the products were opaque and white. However, upon detailed quantitative inspection by optical microscopy, morphometric and colorimetric differences were detected amongst the pellets in their projected perimeter and area, circularity and aspect ratio, and hue, saturation, and brightness (**Figures S1-S7**).

The moldable plastics were determined to be PCL or thermoplastic polyurethane (TPU) by IR spectroscopy (**Figure 1B**). Five plastics were identified as PCL based on spectral matching to reference spectra (Pearson's r >0.96) (**Figures S8-S12**). The remaining seven plastics had IR spectra that matched the reference spectra of thermoplastic polyurethane (TPU) (Pearson's r >0.95) (**Figures S13-S19**). The IR spectra of these samples had a weak νNH stretching vibration at ~3350 cm^{-1}, a shouldering amide I band at ~1685 cm^{-1}, an amide II band at ~1530 cm^{-1}, and νC–O and νC–O–C vibrations at ~1310 cm^{-1} and ~1260 cm^{-1}, respectively, peaks characteristic of polyurethanes.[50] The carbon, hydrogen, and nitrogen content of selected plastics provided additional support to the TPU identification. Those identified as TPU by IR spectroscopy contained bulk nitrogen and had ratios of H/C less than expected for PCL (**Table 1**). Reanalyzing the morphometrics and colorimetrics with respect to polymer type instead of product identified features that distinguished PCL and TPU moldable plastic pellets from one another (**Figure S20**). Notably, the combination of a pellet's aspect ratio and brightness robustly discriminated whether the pellet was PCL or TPU (**Figure S21**).

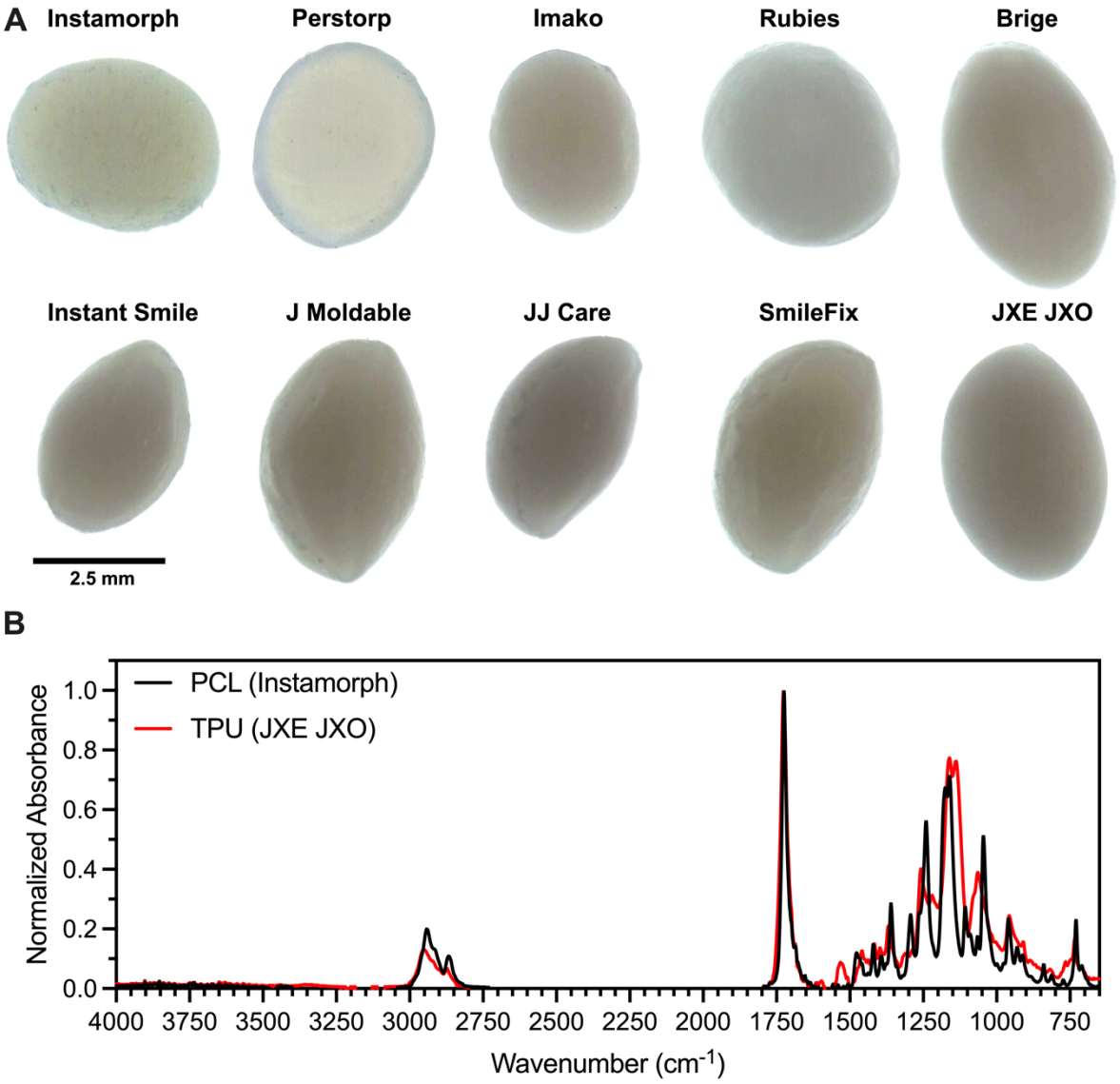

Figure 1. (**A**) Representative microscopy images of the moldable plastic pellets for each product. (**B**) Representative IR spectrum of a PCL-based moldable plastic pellet (Instamorph) and a TPU-based moldable plastic pellet (JXE JXO).

Three modeling plastics accurately reported their polymer type (**Table 1**). Only one of the plastics advertised for oral prosthetics specified their polymer type (**Table 1**). Two plastics, including one sold for dental applications, were incorrectly specified as PCL by the manufacturer; these misreported plastics were determined to be TPU (**Figures S14**, **S16**). We suspect that the products identified as TPU are polycaprolactone-based TPUs in which a polycaprolactone polyol

was used as the chain extender or soft segment in the TPU. This may explain, to some extent, the misreporting and incomplete reporting of the materials underlying these products. Regardless, without detailed chemical analysis or quantitative microscopy, distinguishing whether a product is TPU or PCL is infeasible, leaving consumers largely uninformed about the materials they are buying and potentially putting in their bodies.

Table 1. Survey of several moldable plastics on the market.

Product[a]	Use	Form	# of Ratings[b]	SDS Readily Available	Bulk Elemental Analysis %C	%H	%N	H/C[c]	IR Polymer Assignment[d]	Polymer Specified by Vendor
Instamorph	Consumer	Pellet	12250	Yes	63.96	8.93	0.00	1.66	PCL (S9)	PCL
JXE JXO	Consumer	Pellet	4638	No	60.06	7.83	0.70	1.55	TPU (S15)	Unspecified
uxcell	Consumer	Filament	5	No	61.16	8.06	1.16	1.57	TPU (S16)	PCL
Polly Plastic	Consumer	Sheet	3359	Yes	Not measured				PCL (S11)	PCL
Perstorp	Consumer	Pellet	2	Yes	Not measured				PCL (S10)	PCL
Rubies	Dental	Pellet	562	No	63.77	9.02	0.55	1.69	PCL (S13)	Unspecified
InstantSmile	Dental	Pellet	9977	No	61.20	8.08	1.05	1.57	TPU (S17)	Unspecified
Imako	Dental	Pellet	563	No	64.06	9.00	0.49	1.67	PCL (S12)	Unspecified
SmileFix	Dental	Pellet	699	No	61.31	8.10	1.39	1.57	TPU (S18)	PCL
JJ Care	Dental	Pellet	34	No	61.23	8.08	2.07	1.57	TPU (S19)	Unspecified
Brige	Dental	Pellet	2414	No	Not measured				TPU (S20)	Unspecified
J Moldable	Dental	Pellet	115	No	Not measured				TPU (S21)	Unspecified

[a]Those in bold were tested for toxicity and bioactivity.
[b]On Amazon.com as of 6/29/2023
[c]The theoretical value of H/C for PCL is 1.67; Purasorb PC17 (biomedical-grade PCL) was used as a PCL standard and had a value for H/C of 1.68. Pure PCL is expected to be devoid of N.
[d]Text in parentheses indicates the figure number of the product's IR spectrum.

Consumer-grade PCL can be acutely toxic to developing zebrafish

We evaluated the potential toxicity of two moldable plastic products sold on Amazon.com (Instamorph and JXE JXO pellets) by directly exposing zebrafish embryos to them. These products were selected because they were the most popular consumer moldable plastics included in our survey, and consumers mentioned using them for dental applications in their reviews. For clarity in the subsequent sections, the Instamorph and JXE JXO pellets will be referred to as consumer-grade PCL and TPU, respectively.

No mortality was observed for embryos exposed to ~60 mg/mL (4 pellets/mL) of consumer-grade TPU. Conversely, ~60% of embryos perished within 24 h of continuous exposure to the same concentration of consumer-grade PCL (**Figure 2A**). No changes in mortality for the consumer-grade TPU-treated embryos were observed for the remainder of the exposure experiment (through 72 hpf). Given the significant acute toxicity caused by the consumer-grade PCL and the lack of acute toxicity caused by the consumer-grade TPU, we focused our investigation on the consumer-grade PCL. No further experiments were conducted with the consumer-grade TPU. Nonetheless, there remains potential for the consumer-grade TPU to elicit bioactivity and cause sublethal effects, as polyurethanes have been shown to leach bioactive compounds.[1–3] Further evaluation of TPU-based moldable plastics, particularly those sold for dental applications, is warranted.

We completed several additional exposure experiments using the consumer-grade PCL to determine its toxicity to developing zebrafish in more detail. Embryo mortality followed a sigmoidal-like concentration dependence with an LC_{50} of ~30 mg/mL (2 pellets/mL) (**Figure 2B**). There was no statistical difference in embryo susceptibility to the consumer-grade PCL when exposure to ~60 mg/mL (4 pellets/mL) began at 4, 24, or 48 hpf (**Figure 2C**). A replicated

independent experiment at the LC_{50} concentration affirmed the observed acute toxicity for the consumer-grade PCL (**Figure S22**).

We hypothesized that the consumer-grade PCL was releasing some toxicant(s). To test this, we leached 4 pellets/mL of the consumer-grade PCL for 24 h at room temperature in zebrafish embryo medium and exposed embryos to the resulting leachate. The leachate was slightly more toxic than direct exposure to the pellets and displayed less variability (**Figure 2D**). We also exposed embryos to the pellets used to prepare the leachate ("pre-leached"). Mortality was delayed somewhat for embryos exposed to these pellets, i.e., pre-leaching the pellets appeared to reduce the toxicity of the consumer-grade PCL, at least initially.

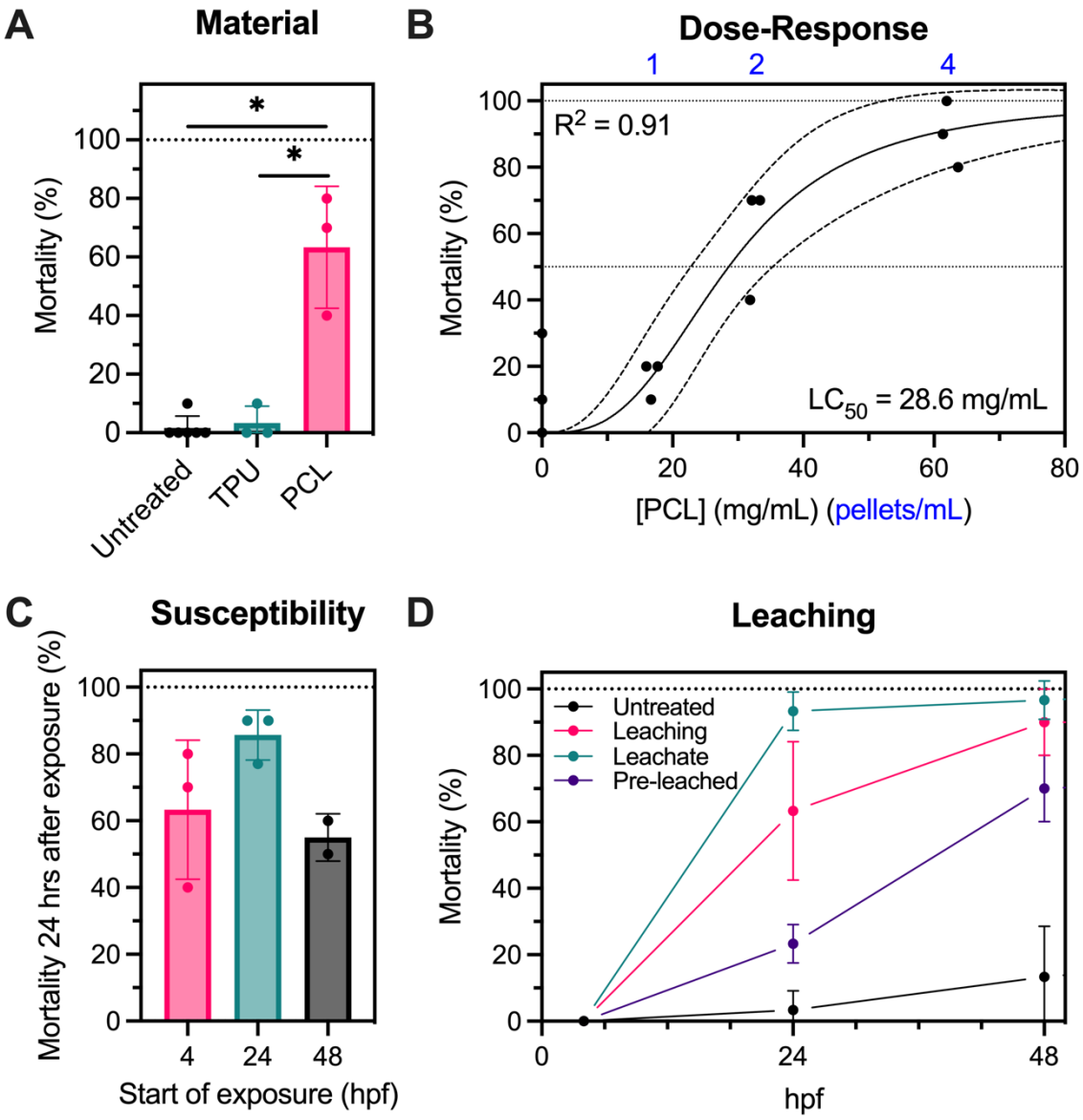

Figure 2. (**A**) Mortality of zebrafish embryos at 24 hpf after a 20 h exposure to 4 pellets/mL of consumer-grade PCL or TPU. Exposures of each material were conducted independently with their own untreated controls. In the figure, the untreated condition presents data combined from both exposures. Statistical differences were determined by Welch's t-test. * corresponds to a *p* value <0.05. (**B**) Dose-response relationship for mortality of zebrafish embryos continuously exposed to consumer-grade PCL from 4-48 hpf. Data were fit to a two-parameter normalized Hill equation, $(\text{Mortality }(\%) = \frac{100}{1+\left(\frac{EC_{50}}{[PCL]}\right)^{n}})$. Residuals were normally distributed and homoscedastic. Dashed lines indicate 95% confidence intervals. (**C**) Mortality of zebrafish embryos after 24 h of exposure to 4 pellets/mL of consumer-grade PCL starting at different stages of development. Treatments were not statistically different as determined by an ordinary one-way ANOVA with Tukey's test for multiple comparisons. (**D**) Mortality of zebrafish embryos exposed to consumer-grade PCL leachate, 4 pellets/mL (leaching), or 4 pre-leached pellets/mL. Each treatment was assessed using three biological replicates unless otherwise noted.

Bioactivity and chemical characterization of consumer-grade PCL-associated chemicals

In parallel to the zebrafish embryo bioassays, we prepared methanolic extracts of the consumer-grade PCL to screen the bioactivity and composition of plastic-associated chemicals using high-throughput *in vitro* bioassays and non-targeted GC×GC analyses, respectively. Methanolic extracts from consumer plastics have proved instructive for assessing the toxic potential of leachable plastic-associated chemicals.[1,3] Additionally, analyses of solvent-extractable material are routine components of food-contact and medical device regulatory frameworks.[18] Blank-corrected methanolic extractable mass for the consumer-grade PCL was 6.59 ± 4.16 mg/g PCL (n=3). The variability in extractable content (coefficient of variation = ~63%) provides a possible explanation for some of the variability observed in the zebrafish bioassays. Due to pellet variability, replicates with lower mortality could have been exposed to pellets with less leachable content and vice-versa.

High-throughput in vitro bioassays.

The TF-FACTORIAL and NR-FACTORIAL *in vitro* bioassays were used to measure the activation of 45 human transcription factor response elements and 24 nuclear receptors, respectively.[22] With these assays, specific biological responses yield unique bioassay profiles that can be used to identify potential modes of action.[20] These assays were conducted using, at most, 216 µg PCL extractable mass/mL (~7-8 mg PCL equivalent mass/mL; ~0.5 equivalent pellets/mL). Screens for cytotoxicity are routinely performed prior to the FACTORIAL bioassays,[20,36] no cytotoxicity was observed for the assayed concentrations of the PCL extracts. Of the 69 endpoints measured, only five were activated within the range of concentrations tested. The activities of all other response elements and receptors were well below an operationally defined 1.5 fold-induction cut-off.

Results were consistent across three extracts prepared from three independent sets of plastic. All activities of the extraction blank were below the induction cut-off (**Figure S23**).

The five endpoints that were activated by the extracts included the TF and NR endpoints for the pregnane X receptor (PXR/PXRE), the TF and NR endpoints for the peroxisome proliferator activated receptor γ (PPARγ/PPRE), and the only endpoint for the nuclear factor erythroid 2-related factor 2 (NRF2) (**Figure 3**, **Tables S5-S6**). The dose-response relationship of PXRE appeared to follow a bell shape, being more stimulatory at lower concentrations than at higher concentrations of the extract (**Figure 3B**, **Table S6**). The dose-response of PPRE and NRF2 appeared sigmoidal within the range of concentrations tested (**Figure 3C-D**, **Table S6**). The elevated activity of PXR/PXRE and PPARγ/PPRE in both TF and NR assays suggested that active components of the extracts acted as direct ligands of PXR and PPARγ. The extent of activation of PXR/PXRE, PPARγ/PPRE, and NRF2 for the 3 µL extract/mL concentration tested were 88%/20%, 6%/19%, and 18% of their positive controls, 10 µM rifampicin (an antibiotic), 1 µM rosiglitazone (an antidiabetic drug), and 100 µM diquat dibromide (an herbicide), respectively.[22,36,51] PXR is touted as a master xenobiotic receptor that is activated by a wide variety of structurally diverse compounds,[52] so its activation in the FACTORIAL bioassays was not surprising. The co-activation of PPARγ and NRF2 suggests that the PCL extracts might perturb lipid metabolism and cause oxidative stress.

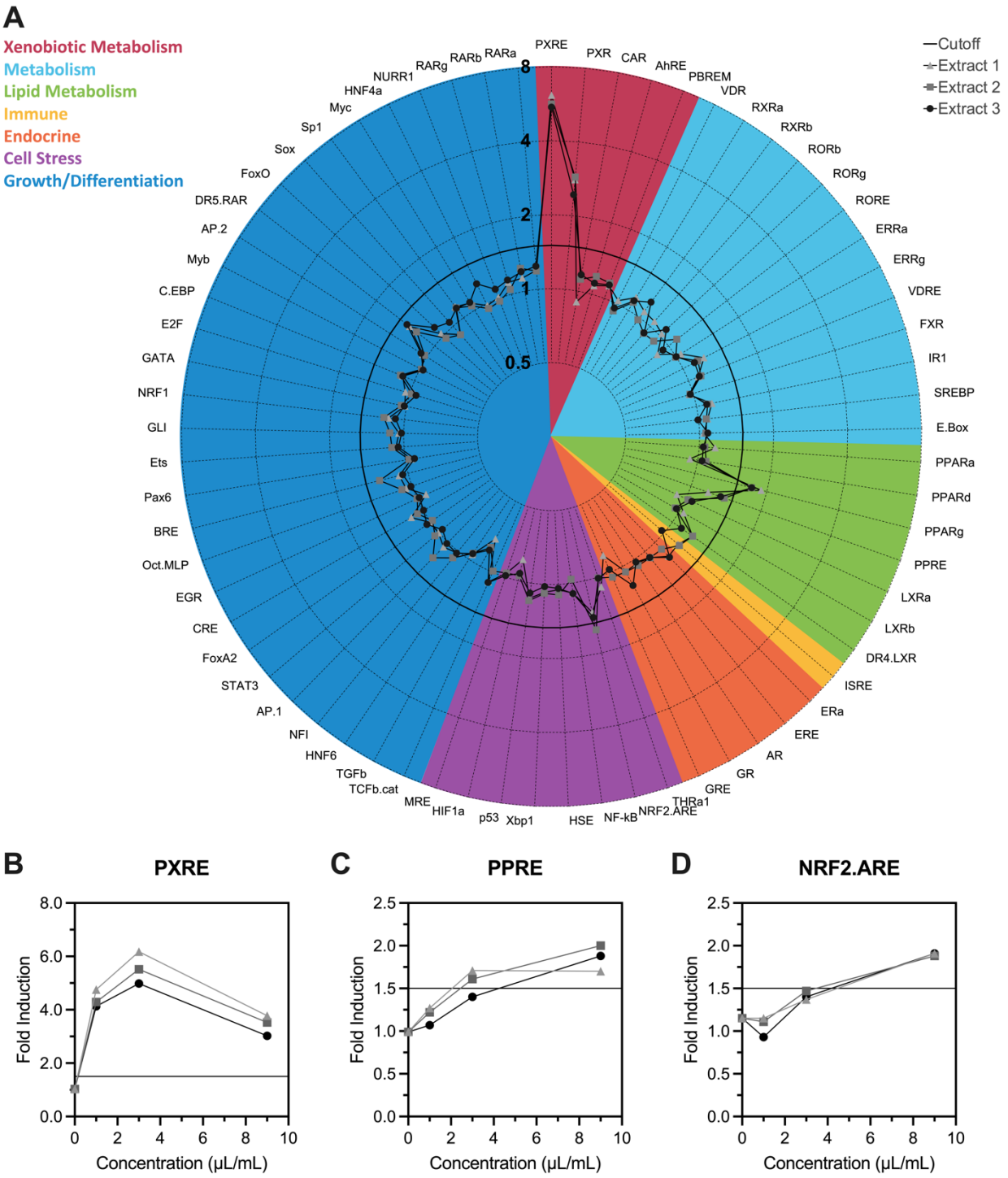

Figure 3. TF-FACTORIAL and NR-FACTORIAL endpoints for consumer-grade PCL methanolic extracts assayed at 3 µL DMSO reconstituted extract/mL cell culture medium (A). Fold induction of all 45 human transcription factor response elements and 24 nuclear receptors tested for activity in the bioassays are included in **Table S5**. Endpoints were grouped and color-coded by biological role.[36] Dose-response relationships of the three extracts for PXRE (B), PPRE (C), and NRF2.ARE (D) at concentrations of 1-9 µL DMSO reconstituted extract/mL cell culture medium. The values at zero concentration were those of the extraction blank (n=1).

Non-targeted GC×GC analyses.

GC×GC-HRT was used to tentatively identify and gauge the relative abundance of chemicals associated with the consumer-grade PCL.[39] This approach chromatographically separates components relative to their vapor pressure and polarity, yielding ordered two-dimensional chromatograms with a high-resolution mass spectrum for each peak.[38] The GC×GC-HRT chromatogram of the methanol extract contained 11 peaks that can broadly be binned into two elution windows. Peaks 1 through 6 were grouped in a narrow band with limited retention in both dimensions. Peaks 7 through 11 eluted along a wide range of retention times.

Peaks 1 and 2 were tentatively identified as 2,6-diisopropylphenyl isocyanate (Peak 1; **Figure 4**, **Figure S24**; CAS# 28178-42-9) and 2,6-diisopropylaniline (Peak 2; **Figure 4**, **Figure S25**; CAS# 24544-04-5). Peaks 5 and 6 shared spectral features with Peaks 1 and 2 (e.g., fragments indicative of a 2,6-diisopropylphenyl unit) and shared fragments indicative of amide bonding (**Figures S28-S29**). The tentative occurrence of isocyanates, anilines, and amides on a 2,6-diisopropylphenyl structural unit likely indicates that these relate to bis(2,6-diisopropylphenyl)carbodiimide (CAS# 2162-74-5),[53] an anti-hydrolysis additive used for polyester stabilization.[54,55] Carbodiimides react with carboxylic acids to form *N*-acylureas that can fragment into amides and isocyanates at elevated temperatures (such as during melt processing).[53] In particular, the absence of bis(2,6-diisopropylphenyl)carbodiimide and the presence of 2,6-diisopropylphenyl isocyanate and 2,6-diisopropylaniline agrees with previous reports on the presence of the compound in plastic leachates.[56] Peak 3 was tentatively identified as methyl 7-oxabicyclo[4.1.0]heptane-3-carboxylate (**Figure 4**, **Figures S26**; CAS# 41088-52-2). Cycloaliphatic epoxides are commonly used as hardeners/crosslinkers with PCL.[57,58] Peak 9 was tentatively identified as 4,4′-butylidenebis(3-methyl-6-*t*-butylphenol) (**Figure 4**, **Figure S32**; CAS# 85-60-9), a phenolic antioxidant used to prevent thermal degradation during melt processing of

polymers. The remaining five peaks (peaks 4, 7, 8, 10, and 11; **Figure 4**, **Figures S27, S30-S31, S33-S34**) were tentatively identified as PCL oligomers owing to their base ion of m/z 115.071 ($C_6H_{11}O_2^+$) and regular addition of m/z 114 with later eluting peaks.[59] Additionally, these peaks formed a "fairway" in the GC×GC chromatogram, a typical chromatographic feature for compounds of the same class with increasing molecular weight.[38] These results reinforce that plastics are not exclusively single compounds but are diverse, complex mixtures of many known and unknown compounds.[4,60]

Previous work has shown that extractables from commercially produced PCL can include ε-caprolactone (CAS# 502-44-3), 6-hydroxyhexanoic acid (CAS# 1191-25-9), and phthalates (unspecified).[61,62] One of the most conventional synthesis routes of PCL uses stannous 2-ethylhexanoate (CAS# 301-10-0) as a catalyst for the ring-opening polymerization of ε-caprolactone.[63] Residual ε-caprolactone, 6-hydroxyhexanoic acid, 2-ethylhexanoic acid (CAS# 149-57-5), and phthalates were not detected.

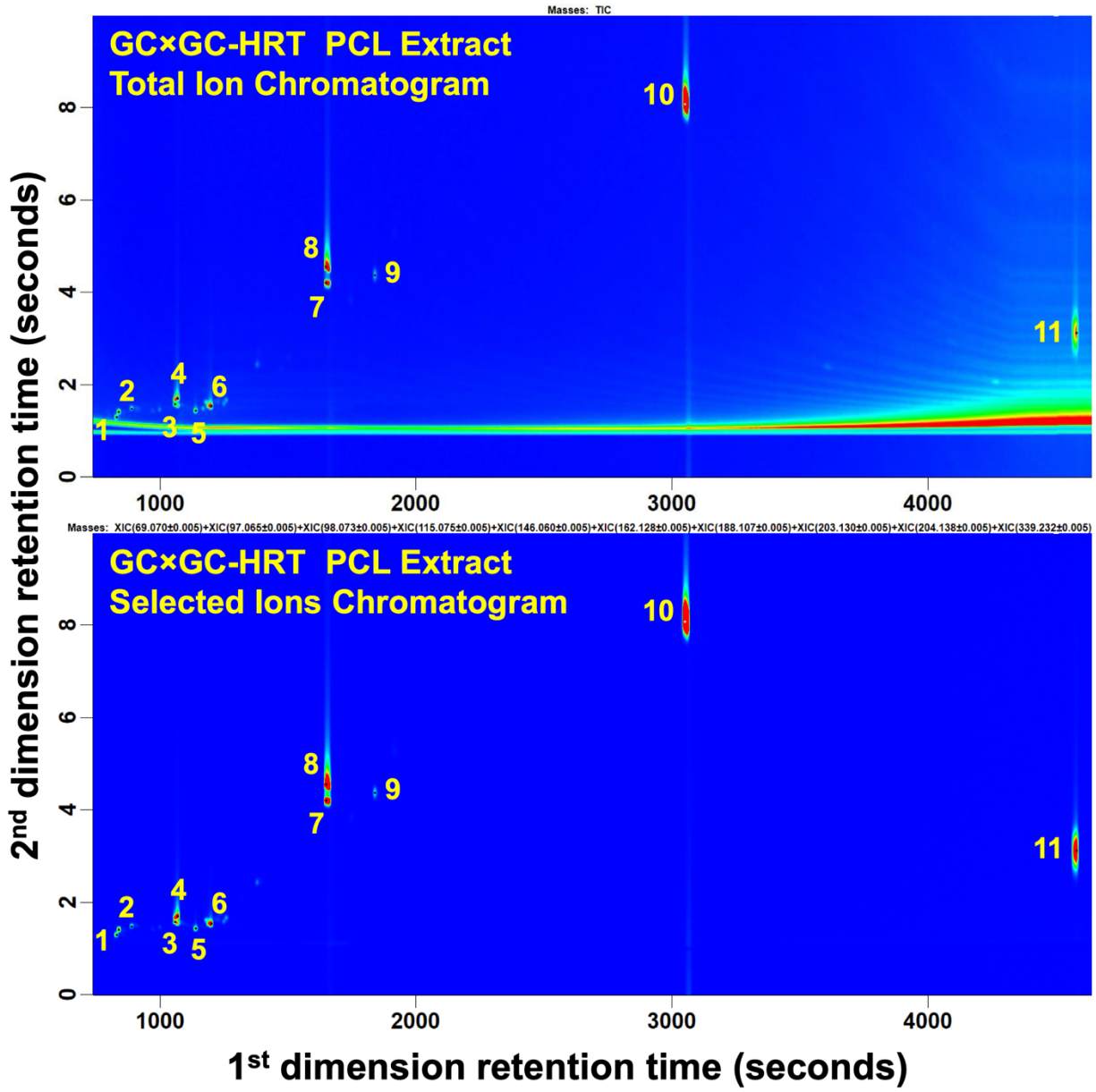

Figure 4. GC×GC-HRT total ion (top) and selected ion (bottom) chromatograms. Selected ions included m/z 97.065, 98.073, 115.075, 146.060, 162.128, 188.107, 203.130, 204.138, and 339.232. A high-resolution mass spectrum for each peak is included in the **Supporting Information**.

High purity biomedical-grade PCL was acutely toxic to zebrafish embryos.

Given the presence of several concerning compounds and those unidentified in the consumer-grade PCL extracts, we hypothesized that the acute toxicity of the consumer-grade PCL to developing zebrafish embryos could be due to these impurities and additives. In a follow-up experiment, we tested biomedical grade PCL for its toxicity to zebrafish embryos in an effort to reduce any confounding effects from leachable chemical additives. Because residual tin catalysts can reduce the biocompatibility of PCL-based biomedical implants,[64] biomedical-grade PCL is purified to reduce residual tin below 50 ppm.[64] Purification presumably also removes residual catalysts and other non-intentionally added substances. If the acute toxicity persisted for this material, it would suggest that components intrinsic to the polymer, i.e., nanoplastics and oligomers, were more likely the cause of toxicity than chemical additives. To test this, we evaluated the toxicity of a commercially available biomedical-grade PCL certified to have residual tin content of 18 ppm, residual monomer content ≤0.5%, and other elemental impurities ≤10 ppm by the United States Pharmacopeial method 232. Dosed at the greatest plastic concentration for consumer-grade PCL tested (~60 mg/mL), we observed an ~80% mortality of zebrafish embryos within 3 dpf when directly exposed to biomedical-grade PCL (**Figure 5**). These results indicated that the observed acute toxicity for PCL was unlikely to be from a chemical additive, residual catalyst, or non-intentionally added substance and suggested that polymer breakdown products (i.e., nanoplastics and oligomers) were the source of the toxicity.

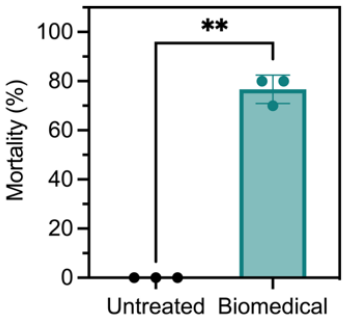

Figure 5. Mortality of zebrafish embryos at 72 hpf after ~3 days of exposure to biomedical-grade PCL (~60 mg/mL). Statistical significance was determined by an unpaired Welch's t test. ** corresponds to a *p* value <0.01.

DISCUSSION

Despite the LC_{50} for consumer-grade PCL (30 mg/mL) being well above the concentration of plastic found in natural waters (~10s ng/L to ~100s mg/L; <100 particles/L),[28] the acute toxicity of PCL raises concern. This is because any mortality of zebrafish embryos from exposure to relatively large pieces of plastic compared to the size of the embryos is rare. For instance, toxicity studies using zebrafish embryos are often conducted in polystyrene well plates because of the material's apparent inertness. Similarly, in an experiment complementary to those presented here, we observed no acute toxicity to zebrafish embryos upon exposure to polyethylene pellets (unpublished data). Based on the results of our chemical analyses and bioassays, supporting evidence in the literature, and additional arguments (see the following section), we suggest that the likely source of the observed acute toxicity of developing zebrafish embryos caused by passive, water-borne exposure to macroscopic PCL was its potentially rapid release of nanoplastics and oligomers within 24 h and thereafter.

It should be noted that the differences in toxic outcomes between our study and previous *in vivo* studies of PCL biomaterials likely stem from differences in local concentration, material properties,

exposure route, matrix composition, and the model organism used and its developmental stage. Our study passively exposed early-developing fish embryos to a relatively high concentration of macroscopic unmodified PCL. In contrast, *in vivo* biomedical studies have implanted or injected engineered PCL biomaterials into developed (adult) mammals.[65–73] Thus, the conditions used to test the biocompatibility of PCL medical devices are not analogous to those used in our study. Because of this, the mechanisms of toxicity relevant to our study could have been missed or gone unrecognized previously. In light of this and the broad use of PCL as a biomaterial, understanding in more detail the source of its acute toxicity to zebrafish is warranted, the study of which can benefit from bringing together biomaterial scientists and environmental scientists.[74] Further investigations of sublethal and chronic exposures to PCL and its breakdown products (e.g., using transgenic lines and transcriptomics) should be pursued to understand the mechanism for its adverse bioactivity, emphasizing pathways related to xenobiotic metabolism, lipid metabolism, and oxidative stress.

Potential explanations for the acute toxicity of consumer-grade PCL to early developing zebrafish

Chemical additives.

Acute toxicity from plastic items is often attributed to the leaching of toxic additives, which include non-intentionally added substances such as reaction by-products.[60] One value of the TF-FACTORIAL and NR-FACTORIAL platforms is that they are part of the U.S. Environmental Protection Agency (EPA) ToxCast program[75] and have been used to screen >3500 compounds, of which a significant portion are also part of the multi-agency Tox21 program.[76] This extensive database presumably enables these platforms to help narrow the number of compounds potentially responsible for toxicity in a complex mixture. As a first pass, we compared the results

of the bioassays to those available on the U.S EPA CompTox dashboard[77] for the compounds tentatively identified by GC×GC in the consumer-grade PCL.

According to the dashboard, 2,6-diisopropylaniline can elicit activity of PXR and RXRβ.[78] Notably, 2,6-diisopropylaniline has been shown to cause adverse bioactivity.[79] As for 2,6-diisopropylphenyl isocyanate, methyl 7-oxabicyclo[4.1.0]heptane-3-carboxylate, 4,4'-butane-1,1-diylbis(2-*t*-butyl-5-methylphenol), and the other tentatively identified compounds, the dashboard indicated these compounds had not been analyzed by the FACTORIAL bioassays.[80–83] 4,4'-butane-1,1-diylbis(2-*t*-butyl-5-methylphenol) had been screened as part of the Tox21 program, which provided evidence for the activity of several pathways not activated in the FACTORIAL bioassays, discounting its contribution to the observed toxicity as well.[80]

Toxicity data on 2,6-diisopropylphenyl isocyanate, methyl 7-oxabicyclo[4.1.0]heptane-3-carboxylate, and bis(2,6-diisopropylphenyl)carbodiimide were severely limited.[82–84] For instance, there were no bioactivity records on PubChem and the U.S. EPA CompTox dashboard for methyl 7-oxabicyclo[4.1.0]heptane-3-carboxylate.[82] Some carbodiimides used in PCL have been shown to be toxic to *Daphnia magna* at concentrations of ~4-8 μM; though, bis(2,6-diisopropylphenyl)carbodiimide was not tested.[85] Additionally, this compound has been approved as an additive for plastics used in food-contact applications, indicating to an extent its perceived level of hazardousness.[56] Further comparison of the FACTORIAL bioassay results to the Attagene database of 6000+ compounds yielded no hits with similarity scores greater than 0.75 (**Table S7**), suggesting the bioactivity was derived from compound(s) not in that database or from a mixture of compounds that produced a unique response pattern in the FACTORIAL bioassays.

Nanoplastics and oligomers.

It is well recognized that PCL undergoes hydrolytic degradation and consequently releases breakdown products,[86] implying that breakdown products could be the dominating source of the observed toxicity and bioactivity. As with nanoplastics, oligomers are increasingly being recognized as chemicals of concern for human health and the environment.[87] Tamayo-Belda et al.[88] demonstrated that consumer-grade PCL pellets shed appreciable quantities of nanoplastics (1.7±0.1 mg/g pellet; $2 \cdot 10^9$ particles/g pellet; mean diameter 67±15 nm), small microplastics (0.7±0.2 mg/g pellet; diameter 100-1000 nm), and linear and cyclic oligomers (0.3±0.1 mg/g pellet) within 1 day of incubation in 1 mM potassium phosphate buffer at pH 7 and ~28 ºC. Yoshinaga et al.[89] showed that short (degree of polymerization ~4) PCL oligomers can exhibit adverse effects on freshwater microorganisms (1 µg/mL), marine algae (1 mg/mL), and mammalian cells (1 mg/mL). In contrast, longer oligomers and bulk PCL had no effect at the same concentrations, which were concentrations lower than those used in our study. Similarly, Tamayo-Belda et al.[88] showed that PCL degradation products from PCL pellets adversely affected two freshwater cyanobacteria. Few studies have investigated the zebrafish response to PCL,[90–93] and those that have primarily focused on small particles, not macroscopic items, as in our study. Luis et al.[92] showed that synthesized PCL nanoparticles (mean diameter 329 nm) were acutely toxic to zebrafish embryos with LC_{50} of 168.9 µg/mL at 96 hpf.[57] Another study investigated the toxicity of finely ground PCL particles to developing zebrafish embryos and found no observable effect on mortality; however, this water-borne exposure was conducted at a concentration of 0.2 mg/mL, well below the concentration that acute toxicity was observed by us (150 times less than the LC_{50}).[93] Comparatively, in the same study, *in vitro* cytotoxicity at 10 mg/mL cell culture medium was observed.[93]

Based on these data in the literature, assuming the consumer-grade PCL pellets used in our study released comparable quantities of material, the estimated concentrations of potentially shed

nanoplastics, small microplastics, and oligomers at the LC_{50} for consumer-grade PCL were ~50 µg/mL (~$6{\cdot}10^7$ particles/mL), ~20 µg/mL, and ~10 µg/mL, respectively. The value of 50 µg/mL (~$6{\cdot}10^7$ particles/mL) is comparable to the LC_{50} for PCL nanoparticles reported by Luis et al. and is likely an underestimate because our exposure conditions were saltier and slightly more basic than those of Tamayo-Belda et al.[88], which can increase PCL degradation.[94] Additionally, nanoparticle biological activity generally increases with decreasing particle size,[95–97] suggesting that the LC_{50} for shed nanoplastics may be lower than the LC_{50} for the synthesized PCL nanoparticles prepared by Luis et al.[92] These studies and our tentative identification of PCL oligomers reinforce the idea that these compounds and other degradation products contributed to the observed toxicity.

The activated endpoints of the FACTORIAL bioassays provided additional evidence for the toxicity resulting from PCL oligomers and nanoplastics. PXR activity further supports the idea that the toxicity to zebrafish embryos was caused by shed nanoplastics and oligomers. While PXR activity can be challenging to interpret, owing to the receptor's ligand binding promiscuity,[98] predictive models of PXR ligands have found that ester groups can be potent activators of human PXR.[99] Because PCL is a polyester, this suggests that PCL breakdown products (i.e., nanoplastics and oligomers) could be the source of bioactivity in the *in vitro* bioassays. The tentative identification of PCL oligomers in the methanolic extracts supports this idea. Because ligands for human and zebrafish PXR are not wholly identical,[100] the activation of zebrafish PXR by PCL and its degradation products will require further investigation. Nonetheless, PXR activity in rats and zebrafish has been reported upon nanoparticle exposure.[101–103] Whether PXR activation is part of the mechanism of toxicity from exposure to PCL pellets is unknown. The primary role of PXR is considered to be in the adaptive regulation of xenobiotic-metabolizing enzymes–i.e., a protective function–but PXR is also involved in regulating lipid and energy

metabolism, and its activation could perturb those processes.[52,104,105] Further research will be needed to assess the significance of the PXR activation seen in our experiments.

The activation of NRF2 suggested that the PCL extracts contained products capable of causing oxidative stress. The oxidative stress response is highly conserved in vertebrates.[106] Embryonic development involves precisely regulated changes in cellular redox balance, and thus, developing embryos are susceptible to chemicals that disrupt redox homeostasis.[107] Numerous studies report evidence of oxidative stress from exposure to plastic particles,[108,109] although the exact components triggering this response are not well understood.

As concern for microplastics and nanoplastics in the body increases, the shedding of particles and oligomers from degradable and non-degradable[110] polymeric implants and their impact on local and systemic biocompatibility requires greater scrutiny. For example, work on another common erodible polymer, polylactic acid (PLA), showed that ingested PLA microplastics can shed nanoplastics and oligomers in the gut, leading to acute inflammation and the translocation of particles from the gut to other tissues.[111] PCL readily degrades in the human body and other environments.[86] Moreover, a recent report by the FDA determined that the systemic effects of PCL-based biomedical implants used clinically are poorly understood.[112] Much of the previous work investigating PCL biocompatibility focused on the polymer's cytocompatibility as measured by routine viability assays (e.g., Microtox, MTT, LDH, and live/dead staining),[113–117] the dynamics of the foreign body response to PCL,[67–72] and the excretion routes of PCL degradation products.[66,73] Few have investigated this polymer's broader bioactivity.[89,118,119] Our finding that PCL extracts can activate nuclear receptors and transcription factors for lipid metabolism and oxidative stress in human cell lines expands this understanding. Previous studies on consumer plastics used in food-contact applications have shown the potential for their plastic-associated chemicals to disrupt endocrine and metabolic signaling.[1–3,5] These studies attributed the observed

bioactivity to extractable chemical additives, while we present evidence that for PCL extracts, the source of their bioactivity and toxicity was likely derived not from chemical additives but from PCL breakdown products (i.e., nanoplastics and oligomers). Future studies should emphasize understanding the toxicity of PCL oligomers and nanoplastics to establish the mechanisms and extent of their bioactivity.

Implications for consumers

For consumers and vendors of PCL-based moldable plastics, our findings conflict with PCL's presumed biological inertness. In recent years, numerous accounts have quantified the release of nanoplastics (or been challenged as having released cyclic oligomers instead[120–123]) from plastic consumer goods, including disposable coffee cups,[124] tea bags,[125,126] baby bottles,[127] rubber teats,[128] and polyester textiles.[129–131] Based on the number of reviews of these products and their content, many users have enjoyed having a low-cost, over-the-counter solution for their dental challenges, particularly when practiced dentistry may be out of reach. A market for these products is unsurprising as it is estimated that ~52% of Americans are missing at least one tooth.[132] Regardless, consumers deserve transparency about the products they purchase to make an informed decision, particularly regarding their health and choice of treatment. As listed on an SDS of a PCL-based moldable plastic,[45,47,48] "The polymer is not bioavailable because of its molecular size." This statement and view of plastic require revision in the context of released nanoplastics, oligomers, and additives from plastic items and the mounting evidence supporting the environmental and human health impacts of plastics.[4]

CONCLUSIONS

This work began by investigating moldable plastics, products with little information available to consumers on their composition and safety that have direct potential for human and environmental exposures. These products were identified as either PCL or TPU. We observed toxic effects in developing zebrafish directly exposed to PCL-based moldable plastics. Initial assessments of the potential sources of toxicity suggested that released nanoparticles and oligomers were responsible. Further study is needed to determine the mechanism of toxicity and if developmental effects occur in zebrafish embryos at sublethal concentrations.

Supporting Information Available

The following files are available free of charge,

Extended materials and methods; morphometrics and colorimetrics of moldable plastic pellets (Figures S1 – S7); ATR-FTIR spectra of moldable plastics (Figures S8 – S19); morphometrics and colorimetrics of PCL and TPU-based moldable plastics (Figures S20 – S21); confirmatory zebrafish study of consumer-grade PCL mortality (Figure S22); TF- and NR- FACTORIAL assay of extraction black (Figure S23); GC×GC-HRT mass spectra of chromatographic peaks (Figures S24 – S34) (PDF).

Solvent extract data (Table S1); TF- and NR- FACTORIAL assay endpoint definitions (Table S2); List of products and companies that have 510(k) pre-market notification for Product Code EBG, "Temporary crown and bridge resin." (Table S3); List of products and companies that have 510(k) pre-market notification for Product Code EBF, "Tooth shade resin material." (Table S4); TF- and NR- FACTORIAL assay endpoint data (Table S5-S6); Top library hits for FACTORIAL assay results (Table S7) (XLSX).

Acknowledgments

We thank Erica M. Aguiar (MIT) for her gift of Instamorph moldable plastic that catalyzed this work, Collin P. Ward (WHOI) for his valuable discussion, Anna P. M. Michel (WHOI) and Sarah Youngs (WHOI) for their assistance with IR spectroscopy, and Chesna Mandl (WHOI) for zebrafish care.

Funding

This work was supported by the Postdoctoral Scholar Program at the Woods Hole Oceanographic Institution, with funding provided by the Weston Howland Jr. Postdoctoral Scholarship (BDJ).

Additional support was provided by the WHOI Ocean Vision Fund 2030 (BDJ), the Seaver Institute (CMR), the March Marine Initiative (a program of March Limited, Bermuda) through WHOI's Marine Microplastics Innovation Accelerator program, and the Woods Hole Center for Oceans and Human Health (NIH P01ES028938 and NSF OCE-1840381) (MEH).

Notes

The authors declare the following competing financial interest(s): A.V.M. and S.S.M. have competing financial interests as Attagene shareholders. The authors declare no other competing interests.

References

(1) Völker, J.; Ashcroft, F.; Vedøy, Å.; Zimmermann, L.; Wagner, M. Adipogenic Activity of Chemicals Used in Plastic Consumer Products. *Environ Sci Technol* **2022**, *56* (4), 2487–2496. https://doi.org/10.1021/acs.est.1c06316.

(2) Zimmermann, L.; Dierkes, G.; Ternes, T. A.; Völker, C.; Wagner, M. Benchmarking the in Vitro Toxicity and Chemical Composition of Plastic Consumer Products. *Environ Sci Technol* **2019**, *53* (19), 11467–11477. https://doi.org/10.1021/acs.est.9b02293.

(3) Zimmermann, L.; Bartosova, Z.; Braun, K.; Oehlmann, J.; Völker, C.; Wagner, M. Plastic Products Leach Chemicals That Induce *In Vitro* Toxicity under Realistic Use Conditions. *Environ Sci Technol* **2021**, *55* (17), 11814–11823. https://doi.org/10.1021/acs.est.1c01103.

(4) Landrigan, P. J.; Raps, H.; Cropper, M.; Bald, C.; Brunner, M.; Canonizado, E. M.; Charles, D.; Chiles, T. C.; Donohue, M. J.; Enck, J.; Fenichel, P.; Fleming, L. E.; Ferrier-Pages, C.; Fordham, R.; Gozt, A.; Griffin, C.; Hahn, M. E.; Haryanto, B.; Hixson, R.; Ianelli, H.; James, B. D.; Kumar, P.; Laborde, A.; Law, K. L.; Martin, K.; Mu, J.; Mulders, Y.; Mustapha, A.; Niu, J.; Pahl, S.; Park, Y.; Pedrotti, M.-L.; Pitt, J. A.; Ruchirawat, M.; Seewoo, B. J.; Spring, M.; Stegeman, J. J.; Suk, W.; Symeonides, C.; Takada, H.; Thompson, R. C.; Vicini, A.; Wang, Z.; Whitman, E.; Wirth, D.; Wolff, M.; Yousuf, A. K.; Dunlop, S. The Minderoo-Monaco Commission on Plastics and Human Health. *Ann Glob Health* **2023**, *89* (1). https://doi.org/10.5334/aogh.4056.

(5) Stevens, S.; McPartland, M.; Bartosova, Z.; Skåland, H. S.; Völker, J.; Wagner, M. Plastic Food Packaging from Five Countries Contains Endocrine- and Metabolism-Disrupting Chemicals. *Environ Sci Technol* **2024**, *58* (11), 4859–4871. https://doi.org/10.1021/acs.est.3c08250.

(6) McPartland, M.; Stevens, S.; Bartosova, Z.; Vardeberg, I. G.; Völker, J.; Wagner, M. Beyond the Nucleus: Plastic Chemicals Activate G Protein-Coupled Receptors. *Environ Sci Technol* **2024**, *58* (11), 4872–4883. https://doi.org/10.1021/acs.est.3c08392.

(7) Vincoff, S.; Schleupner, B.; Santos, J.; Morrison, M.; Zhang, N.; Dunphy-Daly, M. M.; Eward, W. C.; Armstrong, A. J.; Diana, Z.; Somarelli, J. A. The Known and Unknown: Investigating the Carcinogenic Potential of Plastic Additives. *Environ Sci Technol* **2024**. https://doi.org/10.1021/acs.est.3c06840.

(8) Ritter, S. New Car Smell. *Chemical & Engineering News Archive* **2002**, *80* (20), 45. https://doi.org/10.1021/cen-v080n020.p045.

(9) Sáiz, J.; Gómara, B. Evaluation of Endocrine Disrupting Compounds Migration in Household Food Containers under Domestic Use Conditions. *J Agric Food Chem* **2017**, *65* (31), 6692–6700. https://doi.org/10.1021/acs.jafc.7b02479.

(10) Mitro, S. D.; Dodson, R. E.; Singla, V.; Adamkiewicz, G.; Elmi, A. F.; Tilly, M. K.; Zota, A. R. Consumer Product Chemicals in Indoor Dust: A Quantitative Meta-Analysis of U.S. Studies. *Environ Sci Technol* **2016**, *50* (19), 10661–10672. https://doi.org/10.1021/acs.est.6b02023.

(11) Alin, J.; Hakkarainen, M. Microwave Heating Causes Rapid Degradation of Antioxidants in Polypropylene Packaging, Leading to Greatly Increased Specific Migration to Food Simulants As Shown by ESI-MS and GC-MS. *J Agric Food Chem* **2011**, *59* (10), 5418–5427. https://doi.org/10.1021/jf1048639.

(12) *Is polycaprolactone (moldable plastic) toxic?*. Physics Forum. https://www.physicsforums.com/threads/is-polycaprolactone-moldable-plastic-toxic.992469/ (accessed 2023-11-02).

(13) Howard, S. J. Method for Creating a Temporary Tooth. US8613874B2, December 24, 2013.

(14) Instant Smile. *Original Instant Smile - Medium*. https://instantsmileteeth.com/shop/instant-smile-medium/ (accessed 2023-04-20).
(15) Pennsylvania Center for Dental Implants & Periodontics. *DIY Plastic Beads Are Not Meant For Teeth!* https://www.padentalimplants.com/diy-plastic-beads-are-not-meant-for-teeth/ (accessed 2023-11-29).
(16) Haasch, P.; López, Q. *TikTok users are making DIY dentures out of InstaMorph beads that could cause major gum damage*. Business Insider. https://www.insider.com/tiktok-teeth-tooth-diy-dentures-instamorph-beads-dangerous-risky-safe-2021-1 (accessed 2023-11-29).
(17) United States Food and Drug Administration. *Establishment Registration & Device Listing*. https://www.accessdata.fda.gov/scripts/cdrh/cfdocs/cfRL/rl.cfm (accessed 2023-04-20).
(18) Sussman, E. M.; Oktem, B.; Isayeva, I. S.; Liu, J.; Wickramasekara, S.; Chandrasekar, V.; Nahan, K.; Shin, H. Y.; Zheng, J. Chemical Characterization and Non-Targeted Analysis of Medical Device Extracts: A Review of Current Approaches, Gaps, and Emerging Practices. *ACS Biomater Sci Eng* **2022**, *8* (3), 939–963. https://doi.org/10.1021/acsbiomaterials.1c01119.
(19) Wiesinger, H.; Wang, Z.; Hellweg, S. Deep Dive into Plastic Monomers, Additives, and Processing Aids. *Environ Sci Technol* **2021**, *55* (13), 9339–9351. https://doi.org/10.1021/acs.est.1c00976.
(20) Medvedev, A.; Moeser, M.; Medvedeva, L.; Martsen, E.; Granick, A.; Raines, L.; Zeng, M.; Makarov, S.; Houck, K. A.; Makarov, S. S. Evaluating Biological Activity of Compounds by Transcription Factor Activity Profiling. *Sci Adv* **2018**, *4* (9). https://doi.org/10.1126/sciadv.aar4666.
(21) Romanov, S.; Medvedev, A.; Gambarian, M.; Poltoratskaya, N.; Moeser, M.; Medvedeva, L.; Gambarian, M.; Diatchenko, L.; Makarov, S. Homogeneous Reporter System Enables Quantitative Functional Assessment of Multiple Transcription Factors. *Nat Methods* **2008**, *5* (3), 253–260. https://doi.org/10.1038/nmeth.1186.
(22) Martin, M. T.; Dix, D. J.; Judson, R. S.; Kavlock, R. J.; Reif, D. M.; Richard, A. M.; Rotroff, D. M.; Romanov, S.; Medvedev, A.; Poltoratskaya, N.; Gambarian, M.; Moeser, M.; Makarov, S. S.; Houck, K. A. Impact of Environmental Chemicals on Key Transcription Regulators and Correlation to Toxicity End Points within EPA's ToxCast Program. *Chem Res Toxicol* **2010**, *23* (3), 578–590. https://doi.org/10.1021/tx900325g.
(23) Garcia, G. R.; Noyes, P. D.; Tanguay, R. L. Advancements in Zebrafish Applications for 21st Century Toxicology. *Pharmacol Ther* **2016**, *161*, 11–21. https://doi.org/10.1016/j.pharmthera.2016.03.009.
(24) Horzmann, K. A.; Freeman, J. L. Making Waves: New Developments in Toxicology With the Zebrafish. *Toxicological Sciences* **2018**, *163* (1), 5–12. https://doi.org/10.1093/toxsci/kfy044.
(25) Cao, X.; Xie, W.; Feng, M.; Chen, J.; Zhang, J.; Luo, J.; Wang, Y. Nanoplastic Exposure Mediates Neurodevelopmental Toxicity by Activating the Oxidative Stress Response in Zebrafish (*Danio Rerio*). *ACS Omega* **2024**, *9* (14), 16508–16518. https://doi.org/10.1021/acsomega.4c00231.
(26) Fan, X.; Zhang, D.; Hou, T.; Zhang, Q.; Tao, L.; Bian, C.; Wang, Z. Mitochondrial DNA Stress-Mediated Health Risk to Dibutyl Phthalate Contamination on Zebrafish (*Danio Rerio*) at Early Life Stage. *Environ Sci Technol* **2024**, *58* (18), 7731–7742. https://doi.org/10.1021/acs.est.3c10175.
(27) Ding, Q.; Wang, H. Bisphenol AP Exposure-Induced Inflammatory Response in Zebrafish Embryos Revealed by Transcriptomic Analysis. *Environment & Health* **2024**. https://doi.org/10.1021/envhealth.4c00028.

(28) James, B. D.; Karchner, S. I.; Walsh, A. N.; Aluru, N.; Franks, D. G.; Sullivan, K. R.; Reddy, C. M.; Ward, C. P.; Hahn, M. E. Formulation Controls the Potential Neuromuscular Toxicity of Polyethylene Photoproducts in Developing Zebrafish. *Environ Sci Technol* **2023**, *57* (21), 7966–7977. https://doi.org/10.1021/acs.est.3c01932.
(29) Oskui, S. M.; Diamante, G.; Liao, C.; Shi, W.; Gan, J.; Schlenk, D.; Grover, W. H. Assessing and Reducing the Toxicity of 3D-Printed Parts. *Environ Sci Technol Lett* **2016**, *3* (1), 1–6. https://doi.org/10.1021/acs.estlett.5b00249.
(30) Nejedlá, Z.; Poustka, D.; Herma, R.; Liegertová, M.; Štofik, M.; Smejkal, J.; Šícha, V.; Kaule, P.; Malý, J. Class II Biocompatible E-Shell 300 3D Printing Material Causes Severe Developmental Toxicity in *Danio Rerio* Embryos and Reduced Cell Proliferation *in Vitro* – Implications for 3D Printed Microfluidics. *RSC Adv* **2021**, *11* (27), 16252–16267. https://doi.org/10.1039/D1RA00305D.
(31) Cowger, W.; Steinmetz, Z.; Gray, A.; Munno, K.; Lynch, J.; Hapich, H.; Primpke, S.; De Frond, H.; Rochman, C.; Herodotou, O. Microplastic Spectral Classification Needs an Open Source Community: Open Specy to the Rescue! *Anal Chem* **2021**, *93* (21), 7543–7548. https://doi.org/10.1021/acs.analchem.1c00123.
(32) De Vos, A.; Aluwihare, L.; Youngs, S.; Dibenedetto, M. H.; Ward, C. P.; Michel, A. P. M.; Colson, B. C.; Mazzotta, M. G.; Walsh, A. N.; Nelson, R. K.; Reddy, C. M.; James, B. D. The M/V X-Press Pearl Nurdle Spill: Contamination of Burnt Plastic and Unburnt Nurdles along Sri Lanka's Beaches. *ACS Environmental Au* **2022**, *2* (2). https://doi.org/10.1021/acsenvironau.1c00031.
(33) Morét-Ferguson, S.; Law, K. L.; Proskurowski, G.; Murphy, E. K.; Peacock, E. E.; Reddy, C. M. The Size, Mass, and Composition of Plastic Debris in the Western North Atlantic Ocean. *Mar Pollut Bull* **2010**, *60* (10), 1873–1878. https://doi.org/10.1016/j.marpolbul.2010.07.020.
(34) James, B. D.; de Vos, A.; Aluwihare, L. I.; Youngs, S.; Ward, C. P.; Nelson, R. K.; Michel, A. P. M.; Hahn, M. E.; Reddy, C. M. Divergent Forms of Pyroplastic: Lessons Learned from the M/V *X-Press Pearl* Ship Fire. *ACS Environmental Au* **2022**, *2* (5), 467–479. https://doi.org/10.1021/acsenvironau.2c00020.
(35) Westerfield, M. General Methods for Zebrafish Care. In *The zebrafish book. A guide for the laboratory use of zebrafish (Danio rerio)*; University of Oregon Press: Eugene, OR, 2000.
(36) Blackwell, B. R.; Ankley, G. T.; Bradley, P. M.; Houck, K. A.; Makarov, S. S.; Medvedev, A. V.; Swintek, J.; Villeneuve, D. L. Potential Toxicity of Complex Mixtures in Surface Waters from a Nationwide Survey of United States Streams: Identifying in Vitro Bioactivities and Causative Chemicals. *Environ Sci Technol* **2019**, *53* (2), 973–983. https://doi.org/10.1021/acs.est.8b05304.
(37) Hoelzer, K.; Sumner, A. J.; Karatum, O.; Nelson, R. K.; Drollette, B. D.; O'Connor, M. P.; D'Ambro, E. L.; Getzinger, G. J.; Ferguson, P. L.; Reddy, C. M.; Elsner, M.; Plata, D. L. Indications of Transformation Products from Hydraulic Fracturing Additives in Shale-Gas Wastewater. *Environ Sci Technol* **2016**, *50* (15), 8036–8048. https://doi.org/10.1021/acs.est.6b00430.
(38) Nelson, R. K.; Gosselin, K. M.; Hollander, D. J.; Murawski, S. A.; Gracia, A.; Reddy, C. M.; Radović, J. R. Exploring the Complexity of Two Iconic Crude Oil Spills in the Gulf of Mexico (Ixtoc I and Deepwater Horizon) Using Comprehensive Two-Dimensional Gas Chromatography (GC × GC). *Energy & Fuels* **2019**, *33* (5), 3925–3933. https://doi.org/10.1021/acs.energyfuels.8b04384.
(39) Kivenson, V.; Lemkau, K. L.; Pizarro, O.; Yoerger, D. R.; Kaiser, C.; Nelson, R. K.; Carmichael, C.; Paul, B. G.; Reddy, C. M.; Valentine, D. L. Ocean Dumping of Containerized DDT Waste Was a Sloppy Process. *Environ Sci Technol* **2019**, *53* (6), 2971–2980. https://doi.org/10.1021/acs.est.8b05859.

(40) Reddy, C. M.; Nelson, R. K.; Hanke, U. M.; Cui, X.; Summons, R. E.; Valentine, D. L.; Rodgers, R. P.; Chacón-Patiño, M. L.; Niles, S. F.; Teixeira, C. E. P.; Bezerra, L. E. A.; Cavalcante, R. M.; Soares, M. O.; Oliveira, A. H. B.; White, H. K.; Swarthout, R. F.; Lemkau, K. L.; Radović, J. R. Synergy of Analytical Approaches Enables a Robust Assessment of the Brazil Mystery Oil Spill. *Energy & Fuels* **2022**, *36* (22), 13688–13704. https://doi.org/10.1021/acs.energyfuels.2c00656.
(41) U.S. Food and Drug Administration. *21 C.F.R. § 872.3770 Temporary Crown and Bridge Resin.*; United States of America, 2023. https://www.ecfr.gov/current/title-21/part-872/section-872.3770 (accessed 2023-11-29).
(42) U.S. Food and Drug Administration. *21 C.F.R. § 872.3690 Tooth Shade Resin Material.*; United States of America, 2023. https://www.ecfr.gov/current/title-21/part-872/section-872.3690 (accessed 2023-11-29).
(43) United States Food and Drug Administration. *Are There "FDA Registered" or "FDA Certified" Medical Devices? How Do I Know What Is FDA Approved?* https://www.fda.gov/medical-devices/consumers-medical-devices/are-there-fda-registered-or-fda-certified-medical-devices-how-do-i-know-what-fda-approved (accessed 2023-06-28).
(44) U.S. Food and Drug Administration. *510(k) Premarket Notification*. https://www.accessdata.fda.gov/scripts/cdrh/cfdocs/cfPMN/pmn.cfm (accessed 2023-11-29).
(45) Thermoworx. Whitemorph MSDS. https://www.homesciencetools.com/content/reference/SU-MATWOR.pdf (accessed 2023-02-26).
(46) American Art Clay Co Inc. Friendly Plastic Pellets Ivory Safety Data Sheet. 2016. https://www.lmii.com/blog/wp-content/uploads/2018/03/CFP.pdf (accessed 2023-02-26).
(47) Polly Plastics. Polly Plastics Safety Data Sheet. 2016. https://s3-eu-west-1.amazonaws.com/s3-euw1-ap-pe-ws4-cws-documents.ri-prod/9781138212275/safety/polypellets.pdf (accessed 2023-02-26).
(48) Instamorph. Moldable Plastic Material Safety Data Sheet. 2015. https://cdn.shopify.com/s/files/1/0615/5901/3537/files/20220814_InstaMorph_MSDS_updated.pdf?v=1671634714 (accessed 2023-02-26).
(49) Amazon.com. *Customer reviews Moldable Plastic Thermoplastic Beads 8OZ*. https://www.amazon.com/Moldable-Plastic-Thermoplastic-Beads-8OZ/product-reviews/B077874HM8/ref=cm_cr_arp_d_viewopt_kywd?ie=UTF8&reviewerType=all_reviews&pageNumber=1&filterByKeyword=instamorph (accessed 2023-02-26).
(50) Corish, P. J. Identification and Analysis of Polyurethane Rubbers by Infrared Spectroscopy. *Anal Chem* **1959**, *31* (8), 1298–1306. https://doi.org/10.1021/ac60152a015.
(51) U.S. Environmental Protection Agency. *Rifampicin*. Comptox Chemicals Dashboard. https://comptox.epa.gov/dashboard/chemical/details/DTXSID6021244 (accessed 2024-06-05).
(52) Oladimeji, P. O.; Chen, T. PXR: More Than Just a Master Xenobiotic Receptor. *Mol Pharmacol* **2018**, *93* (2), 119–127. https://doi.org/10.1124/mol.117.110155.
(53) Chen, A.-L.; Wei, K.-L.; Jeng, R.-J.; Lin, J.-J.; Dai, S. A. Well-Defined Polyamide Synthesis from Diisocyanates and Diacids Involving Hindered Carbodiimide Intermediates. *Macromolecules* **2011**, *44* (1), 46–59. https://doi.org/10.1021/ma1022378.
(54) Stloukal, P.; Jandikova, G.; Koutny, M.; Sedlařík, V. Carbodiimide Additive to Control Hydrolytic Stability and Biodegradability of PLA. *Polym Test* **2016**, *54*, 19–28. https://doi.org/10.1016/j.polymertesting.2016.06.007.

(55) Kim, H.-S.; Kim, H.-J.; Cho, D. Thermal Analysis of Hydrolysis and Degradation of Biodegradable Polymer and Bio-Composites. *J Therm Anal Calorim* **2009**, *96* (1), 211–218. https://doi.org/10.1007/s10973-008-9003-5.
(56) Scientific Opinion on the Safety Evaluation of the Substance Bis(2,6-diisopropylphenyl)Carbodiimide for Use in Food Contact Materials. *EFSA Journal* **2010**, *8* (12). https://doi.org/10.2903/j.efsa.2010.1928.
(57) Lützen, H.; Gesing, T. M.; Kim, B. K.; Hartwig, A. Novel Cationically Polymerized Epoxy/Poly(ε-Caprolactone) Polymers Showing a Shape Memory Effect. *Polymer (Guildf)* **2012**, *53* (26), 6089–6095. https://doi.org/10.1016/j.polymer.2012.10.033.
(58) Arnebold, A.; Thiel, K.; Kentzinger, E.; Hartwig, A. Morphological Adjustment Determines the Properties of Cationically Polymerized Epoxy Resins. *RSC Adv* **2015**, *5* (53), 42482–42491. https://doi.org/10.1039/C5RA03042K.
(59) Lüderwald, I. Über Den Thermischen Abbau Des Poly(E-caprolacton)s. *Die Makromolekulare Chemie* **1977**, *178* (9), 2603–2607. https://doi.org/10.1002/macp.1977.021780911.
(60) Wiesinger, H.; Wang, Z.; Hellweg, S. Deep Dive into Plastic Monomers, Additives, and Processing Aids. *Environ Sci Technol* **2021**, *55* (13), 9339–9351. https://doi.org/10.1021/acs.est.1c00976.
(61) Hakkarainen, M.; Albertsson, A.-C. Heterogeneous Biodegradation of Polycaprolactone – Low Molecular Weight Products and Surface Changes. *Macromol Chem Phys* **2002**, *203* (10–11), 1357–1363. https://doi.org/10.1002/1521-3935(200207)203:10/11<1357::AID-MACP1357>3.0.CO;2-R.
(62) Höglund, A.; Hakkarainen, M.; Albertsson, A. Degradation Profile of Poly(E-caprolactone)–the Influence of Macroscopic and Macromolecular Biomaterial Design. *Journal of Macromolecular Science, Part A* **2007**, *44* (9), 1041–1046. https://doi.org/10.1080/10601320701424487.
(63) Labet, M.; Thielemans, W. Synthesis of Polycaprolactone: A Review. *Chem Soc Rev* **2009**, *38* (12), 3484. https://doi.org/10.1039/b820162p.
(64) Stjerndahl, A.; Finne-Wistrand, A.; Albertsson, A.-C.; Bäckesjö, C. M.; Lindgren, U. Minimization of Residual Tin in the Controlled Sn(II)Octoate-Catalyzed Polymerization of ε-Caprolactone. *J Biomed Mater Res A* **2008**, *87A* (4), 1086–1091. https://doi.org/10.1002/jbm.a.31733.
(65) Pappalardo, D.; Mathisen, T.; Finne-Wistrand, A. Biocompatibility of Resorbable Polymers: A Historical Perspective and Framework for the Future. *Biomacromolecules* **2019**, *20* (4), 1465–1477. https://doi.org/10.1021/acs.biomac.9b00159.
(66) Sun, H.; Mei, L.; Song, C.; Cui, X.; Wang, P. The in Vivo Degradation, Absorption and Excretion of PCL-Based Implant. *Biomaterials* **2006**, *27* (9), 1735–1740. https://doi.org/10.1016/j.biomaterials.2005.09.019.
(67) Bezwada, R. S.; Jamiolkowski, D. D.; Lee, I.-Y.; Agarwal, V.; Persivale, J.; Trenka-Benthin, S.; Erneta, M.; Suryadevara, J.; Yang, A.; Liu, S. Monocryl® Suture, a New Ultra-Pliable Absorbable Monofilament Suture. *Biomaterials* **1995**, *16* (15), 1141–1148. https://doi.org/10.1016/0142-9612(95)93577-Z.
(68) Den Dunnen, W. F. A.; Schakenraad, J. M.; Zondervan, G. J.; Pennings, A. J.; Van Der Lei, B.; Robinson, P. H. A New PLLA/PCL Copolymer for Nerve Regeneration. *J Mater Sci Mater Med* **1993**, *4* (5), 521–525. https://doi.org/10.1007/BF00120133.
(69) Grijpma, D. W.; Zondervan, G. J.; Pennings, A. J. High Molecular Weight Copolymers of L-Lactide and ?-Caprolactone as Biodegradable Elastomeric Implant Materials. *Polymer Bulletin* **1991**, *25* (3), 327–333. https://doi.org/10.1007/BF00316902.
(70) Den Dunnen, W. F. A.; van der Lei, B.; Schakenraad, J. M.; Blaauw, E. H.; Stokroos, I.; Pennings, A. J.; Robinson, P. H. Long-term Evaluation of Nerve Regeneration in a

Biodegradable Nerve Guide. *Microsurgery* **1993**, *14* (8), 508–515. https://doi.org/10.1002/micr.1920140808.
(71) Pogorielov, M.; Hapchenko, A.; Deineka, V.; Rogulska, L.; Oleshko, O.; Vodseďálková, K.; Berezkinová, L.; Vysloužilová, L.; Klápšťová, A.; Erben, J. *In Vitro* Degradation and *in Vivo* Toxicity of NanoMatrix3D ® Polycaprolactone and Poly(Lactic Acid) Nanofibrous Scaffolds. *J Biomed Mater Res A* **2018**, *106* (8), 2200–2212. https://doi.org/10.1002/jbm.a.36427.
(72) Lam, C. X. F.; Hutmacher, D. W.; Schantz, J.; Woodruff, M. A.; Teoh, S. H. Evaluation of Polycaprolactone Scaffold Degradation for 6 Months *in Vitro* and *in Vivo*. *J Biomed Mater Res A* **2009**, *90A* (3), 906–919. https://doi.org/10.1002/jbm.a.32052.
(73) Pitt, C. G.; Chasalow, F. I.; Hibionada, Y. M.; Klimas, D. M.; Schindler, A. Aliphatic Polyesters. I. The Degradation of Poly(ϵ-Caprolactone) *in Vivo*. *J Appl Polym Sci* **1981**, *26* (11), 3779–3787. https://doi.org/10.1002/app.1981.070261124.
(74) James, B. D.; Hahn, M. E.; Reddy, C. M. Biomaterials Science Can Offer a Valuable Second Opinion on Nature's Plastic Malady. *Environ Sci Technol* **2022**, *56* (3). https://doi.org/10.1021/acs.est.1c07569.
(75) Richard, A. M.; Judson, R. S.; Houck, K. A.; Grulke, C. M.; Volarath, P.; Thillainadarajah, I.; Yang, C.; Rathman, J.; Martin, M. T.; Wambaugh, J. F.; Knudsen, T. B.; Kancherla, J.; Mansouri, K.; Patlewicz, G.; Williams, A. J.; Little, S. B.; Crofton, K. M.; Thomas, R. S. ToxCast Chemical Landscape: Paving the Road to 21st Century Toxicology. *Chem Res Toxicol* **2016**, *29* (8), 1225–1251. https://doi.org/10.1021/acs.chemrestox.6b00135.
(76) Richard, A. M.; Huang, R.; Waidyanatha, S.; Shinn, P.; Collins, B. J.; Thillainadarajah, I.; Grulke, C. M.; Williams, A. J.; Lougee, R. R.; Judson, R. S.; Houck, K. A.; Shobair, M.; Yang, C.; Rathman, J. F.; Yasgar, A.; Fitzpatrick, S. C.; Simeonov, A.; Thomas, R. S.; Crofton, K. M.; Paules, R. S.; Bucher, J. R.; Austin, C. P.; Kavlock, R. J.; Tice, R. R. The Tox21 10K Compound Library: Collaborative Chemistry Advancing Toxicology. *Chem Res Toxicol* **2021**, *34* (2), 189–216. https://doi.org/10.1021/acs.chemrestox.0c00264.
(77) Williams, A. J.; Grulke, C. M.; Edwards, J.; McEachran, A. D.; Mansouri, K.; Baker, N. C.; Patlewicz, G.; Shah, I.; Wambaugh, J. F.; Judson, R. S.; Richard, A. M. The CompTox Chemistry Dashboard: A Community Data Resource for Environmental Chemistry. *J Cheminform* **2017**, *9* (1), 61. https://doi.org/10.1186/s13321-017-0247-6.
(78) U.S. Environmental Protection Agency. *2,6-Diisopropylaniline*. Comptox Chemicals Dashboard. https://comptox.epa.gov/dashboard/chemical/details/DTXSID5022279 (accessed 2023-11-03).
(79) Short, C.; King, C.; Sistrunk, P.; Kerr, K. Subacute Toxicity of Several Ring-Substituted Dialkylanilines in the Rat. *Fundamental and Applied Toxicology* **1983**, *3* (4), 285–292. https://doi.org/10.1016/S0272-0590(83)80141-9.
(80) U.S. Environmental Protection Agency. *4,4'-Butane-1,1-diylbis(2-tert-butyl-5-methylphenol)*. Comptox Chemicals Dashboard. https://comptox.epa.gov/dashboard/chemical/details/DTXSID8029602 (accessed 2023-11-03).
(81) U.S. Environmental Protection Agency. *6-Hydroxyhexanoic acid*. Comptox Chemicals Dashboard. https://comptox.epa.gov/dashboard/chemical/details/DTXSID00152316 (accessed 2023-11-03).
(82) U.S. Environmental Protection Agency. *7-Oxabicyclo[4.1.0]heptane-3-carboxylic acid, methyl ester*. Comptox Chemicals Dashboard. https://comptox.epa.gov/dashboard/chemical/details/DTXSID00884680 (accessed 2023-11-29).
(83) U.S. Environmental Protection Agency. *2,6-Diisopropylphenyl isocyanate*. Comptox Chemicals Dashboard.

https://comptox.epa.gov/dashboard/chemical/details/DTXSID9051959 (accessed 2023-11-29).
(84) U.S. Environmental Protection Agency. *Bis(2,6-diisopropylphenyl)carbodiimide*. Comptox Chemicals Dashboard. https://comptox.epa.gov/dashboard/chemical/details/DTXSID5051862 (accessed 2023-11-29).
(85) Matsumoto, M.; Ito, H.; Tateishi, A.; Kobayashi, Y.; Satoh, K.; Numata, K.; Miyakawa, H. Effects of Polycaprolactone Degradation Products on the Water Flea, <scp> *Daphnia Magna* </Scp> : Carbodiimide Additives Have Acute and Chronic Toxicity. *Journal of Applied Toxicology* **2023**, *43* (12), 1840–1848. https://doi.org/10.1002/jat.4516.
(86) Bartnikowski, M.; Dargaville, T. R.; Ivanovski, S.; Hutmacher, D. W. Degradation Mechanisms of Polycaprolactone in the Context of Chemistry, Geometry and Environment. *Prog Polym Sci* **2019**, *96*, 1–20. https://doi.org/10.1016/j.progpolymsci.2019.05.004.
(87) Shi, C.; Wang, M.; Wang, Z.; Qu, G.; Jiang, W.; Pan, X.; Fang, M. Oligomers from the Synthetic Polymers: Another Potential Iceberg of New Pollutants. *Environment & Health* **2023**, *1* (4), 228–235. https://doi.org/10.1021/envhealth.3c00086.
(88) Tamayo-Belda, M.; Pulido-Reyes, G.; González-Pleiter, M.; Martín-Betancor, K.; Leganés, F.; Rosal, R.; Fernández-Piñas, F. Identification and Toxicity towards Aquatic Primary Producers of the Smallest Fractions Released from Hydrolytic Degradation of Polycaprolactone Microplastics. *Chemosphere* **2022**, *303*, 134966. https://doi.org/10.1016/j.chemosphere.2022.134966.
(89) Yoshinaga, N.; Tateishi, A.; Kobayashi, Y.; Kubo, T.; Miyakawa, H.; Satoh, K.; Numata, K. Effect of Oligomers Derived from Biodegradable Polyesters on Eco- and Neurotoxicity. *Biomacromolecules* **2023**, *24* (6), 2721–2729. https://doi.org/10.1021/acs.biomac.3c00160.
(90) Zhang, X.; Stockhammer, Oliver. W.; de Boer, L.; Vischer, Norbert. O. E.; Spaink, Herman. P.; Grijpma, Dirk. W.; Zaat, Sebastian. A. J. The Zebrafish Embryo as a Model to Quantify Early Inflammatory Cell Responses to Biomaterials. *J Biomed Mater Res A* **2017**, *105* (9), 2522–2532. https://doi.org/10.1002/jbm.a.36110.
(91) Tao, J.; Wei, Z.; Xu, M.; Xi, L.; Cheng, Y.; Lee, S. M.; Ge, W.; Zheng, Y. Particle Integrity and Size Effect on the Journey of Polymeric Nanocarriers in Zebrafish Model and the Correlation with Mice. *Small* **2021**, *17* (43), 2103584. https://doi.org/10.1002/smll.202103584.
(92) Luis, A. I. S.; Campos, E. V. R.; Oliveira, J. L.; Vallim, J. H.; Proença, P. L. F.; Castanha, R. F.; de Castro, V. L. S. S.; Fraceto, L. F. Ecotoxicity Evaluation of Polymeric Nanoparticles Loaded with Ascorbic Acid for Fish Nutrition in Aquaculture. *J Nanobiotechnology* **2021**, *19* (1), 163. https://doi.org/10.1186/s12951-021-00910-8.
(93) Ponjavic, M.; Nikolic, M. S.; Stevanovic, S.; Nikodinovic-Runic, J.; Jeremic, S.; Pavic, A.; Djonlagic, J. Hydrolytic Degradation of Star-Shaped Poly(ε-Caprolactone)s with Different Number of Arms and Their Cytotoxic Effects. *J Bioact Compat Polym* **2020**, *35* (6), 517–537. https://doi.org/10.1177/0883911520951826.
(94) Lu, B.; Wang, G.-X.; Huang, D.; Ren, Z.-L.; Wang, X.-W.; Wang, P.-L.; Zhen, Z.-C.; Zhang, W.; Ji, J.-H. Comparison of PCL Degradation in Different Aquatic Environments: Effects of Bacteria and Inorganic Salts. *Polym Degrad Stab* **2018**, *150*, 133–139. https://doi.org/10.1016/j.polymdegradstab.2018.02.002.
(95) Albanese, A.; Tang, P. S.; Chan, W. C. W. The Effect of Nanoparticle Size, Shape, and Surface Chemistry on Biological Systems. *Annu Rev Biomed Eng* **2012**, *14* (1), 1–16. https://doi.org/10.1146/annurev-bioeng-071811-150124.

(96) Kögel, T.; Bjorøy, Ø.; Toto, B.; Bienfait, A. M.; Sanden, M. Micro- and Nanoplastic Toxicity on Aquatic Life: Determining Factors. *Science of The Total Environment* **2020**, *709*, 136050. https://doi.org/10.1016/j.scitotenv.2019.136050.
(97) Park, M. V. D. Z.; Neigh, A. M.; Vermeulen, J. P.; de la Fonteyne, L. J. J.; Verharen, H. W.; Briedé, J. J.; van Loveren, H.; de Jong, W. H. The Effect of Particle Size on the Cytotoxicity, Inflammation, Developmental Toxicity and Genotoxicity of Silver Nanoparticles. *Biomaterials* **2011**, *32* (36), 9810–9817. https://doi.org/10.1016/j.biomaterials.2011.08.085.
(98) Ngan, C.-H.; Beglov, D.; Rudnitskaya, A. N.; Kozakov, D.; Waxman, D. J.; Vajda, S. The Structural Basis of Pregnane X Receptor Binding Promiscuity. *Biochemistry* **2009**, *48* (48), 11572–11581. https://doi.org/10.1021/bi901578n.
(99) AbdulHameed, M. D. M.; Ippolito, D. L.; Wallqvist, A. Predicting Rat and Human Pregnane X Receptor Activators Using Bayesian Classification Models. *Chem Res Toxicol* **2016**, *29* (10), 1729–1740. https://doi.org/10.1021/acs.chemrestox.6b00227.
(100) Creusot, N.; Garoche, C.; Grimaldi, M.; Boulahtouf, A.; Chiavarina, B.; Bourguet, W.; Balaguer, P. A Comparative Study of Human and Zebrafish Pregnane X Receptor Activities of Pesticides and Steroids Using In Vitro Reporter Gene Assays. *Front Endocrinol (Lausanne)* **2021**, *12*. https://doi.org/10.3389/fendo.2021.665521.
(101) Daujat-Chavanieu, M.; Gerbal-Chaloin, S. Regulation of CAR and PXR Expression in Health and Disease. *Cells* **2020**, *9* (11), 2395. https://doi.org/10.3390/cells9112395.
(102) Hu, J.; Tian, J.; Yuan, T.; Yin, Q.; Yin, J. The Critical Role of Nanoparticle Sizes in the Interactions between Gold Nanoparticles and ABC Transporters in Zebrafish Embryos. *Aquatic Toxicology* **2022**, *251*, 106286. https://doi.org/10.1016/j.aquatox.2022.106286.
(103) Tian, J.; Hu, J.; Liu, G.; Yin, H.; Chen, M.; Miao, P.; Bai, P.; Yin, J. Altered Gene Expression of ABC Transporters, Nuclear Receptors and Oxidative Stress Signaling in Zebrafish Embryos Exposed to CdTe Quantum Dots. *Environmental Pollution* **2019**, *244*, 588–599. https://doi.org/10.1016/j.envpol.2018.10.092.
(104) Spruiell, K.; Richardson, R. M.; Cullen, J. M.; Awumey, E. M.; Gonzalez, F. J.; Gyamfi, M. A. Role of Pregnane X Receptor in Obesity and Glucose Homeostasis in Male Mice. *Journal of Biological Chemistry* **2014**, *289* (6), 3244–3261. https://doi.org/10.1074/jbc.M113.494575.
(105) Itkonen, A.; Hakkola, J.; Rysä, J. Adverse Outcome Pathway for Pregnane X Receptor-Induced Hypercholesterolemia. *Arch Toxicol* **2023**, *97* (11), 2861–2877. https://doi.org/10.1007/s00204-023-03575-4.
(106) Hahn, M. E.; Timme-Laragy, A. R.; Karchner, S. I.; Stegeman, J. J. Nrf2 and Nrf2-Related Proteins in Development and Developmental Toxicity: Insights from Studies in Zebrafish (Danio Rerio). *Free Radic Biol Med* **2015**, *88* (Pt B), 275–289. https://doi.org/10.1016/j.freeradbiomed.2015.06.022.
(107) Timme-Laragy, A. R.; Goldstone, J. V; Imhoff, B. R.; Stegeman, J. J.; Hahn, M. E.; Hansen, J. M. Glutathione Redox Dynamics and Expression of Glutathione-Related Genes in the Developing Embryo. *Free Radic Biol Med* **2013**, *65*, 89–101. https://doi.org/10.1016/j.freeradbiomed.2013.06.011.
(108) Khan, A.; Jia, Z. Recent Insights into Uptake, Toxicity, and Molecular Targets of Microplastics and Nanoplastics Relevant to Human Health Impacts. *iScience* **2023**, *26* (2), 106061. https://doi.org/10.1016/j.isci.2023.106061.
(109) Das, A. The Emerging Role of Microplastics in Systemic Toxicity: Involvement of Reactive Oxygen Species (ROS). *Sci Total Environ* **2023**, *895*, 165076. https://doi.org/10.1016/j.scitotenv.2023.165076.
(110) Liu, A.; Richards, L.; Bladen, C. L.; Ingham, E.; Fisher, J.; Tipper, J. L. The Biological Response to Nanometre-Sized Polymer Particles. *Acta Biomater* **2015**, *23*, 38–51. https://doi.org/10.1016/j.actbio.2015.05.016.

(111) Wang, M.; Li, Q.; Shi, C.; Lv, J.; Xu, Y.; Yang, J.; Chua, S. L.; Jia, L.; Chen, H.; Liu, Q.; Huang, C.; Huang, Y.; Chen, J.; Fang, M. Oligomer Nanoparticle Release from Polylactic Acid Plastics Catalysed by Gut Enzymes Triggers Acute Inflammation. *Nat Nanotechnol* **2023**. https://doi.org/10.1038/s41565-023-01329-y.
(112) ECRI. *Polycaprolactone (PCL) Safety Profile*; 2021. https://www.fda.gov/media/158492/download (accessed 2023-02-27).
(113) V.S., S.; P.V., M. Degradation of Poly(ε-Caprolactone) and Bio-Interactions with Mouse Bone Marrow Mesenchymal Stem Cells. *Colloids Surf B Biointerfaces* **2018**, *163*, 107–118. https://doi.org/10.1016/j.colsurfb.2017.12.039.
(114) Reisman, L.; Siehr, A.; Horn, J.; Batiste, D. C.; Kim, H. J.; De Hoe, G. X.; Ellison, C. J.; Shen, W.; White, E. M.; Hillmyer, M. A. Respirometry and Cell Viability Studies for Sustainable Polyesters and Their Hydrolysis Products. *ACS Sustain Chem Eng* **2021**, *9* (7), 2736–2744. https://doi.org/10.1021/acssuschemeng.0c08026.
(115) Taylor, M. S.; Daniels, A. U.; Andriano, K. P.; Heller, J. Six Bioabsorbable Polymers: In Vitro Acute Toxicity of Accumulated Degradation Products. *Journal of applied biomaterials* **1994**, *5* (2), 151–157.
(116) Gong, C.; Gu, Y.; Wang, X.; Yi, C. Oligomer Content Determines the Properties and Application of Polycaprolactone. *Macromolecules* **2022**, *55* (13), 5342–5352. https://doi.org/10.1021/acs.macromol.2c00275.
(117) Brackett, M. G.; Marshall, A.; Lockwood, P. E.; Lewis, J. B.; Messer, R. L. W.; Bouillaguet, S.; Wataha, J. C. Cytotoxicity of Endodontic Materials over 6-weeks *Ex Vivo*. *Int Endod J* **2008**, *41* (12), 1072–1078. https://doi.org/10.1111/j.1365-2591.2008.01471.x.
(118) Cherry, C.; Maestas, D. R.; Han, J.; Andorko, J. I.; Cahan, P.; Fertig, E. J.; Garmire, L. X.; Elisseeff, J. H. Computational Reconstruction of the Signalling Networks Surrounding Implanted Biomaterials from Single-Cell Transcriptomics. *Nat Biomed Eng* **2021**, *5* (10), 1228–1238. https://doi.org/10.1038/s41551-021-00770-5.
(119) Jesus, S.; Bernardi, N.; da Silva, J.; Colaço, M.; Panão Costa, J.; Fonte, P.; Borges, O. Unravelling the Immunotoxicity of Polycaprolactone Nanoparticles—Effects of Polymer Molecular Weight, Hydrolysis, and Blends. *Chem Res Toxicol* **2020**, *33* (11), 2819–2833. https://doi.org/10.1021/acs.chemrestox.0c00208.
(120) Stark, M. Plausibility Checks Are Needed in Microplastic Research to Prevent Misinterpretations. *Environ Sci Technol* **2022**, *56* (24), 17495–17497. https://doi.org/10.1021/acs.est.2c05989.
(121) Stark, M. Comment on “Characterization of Nanoplastics, Fibrils, and Microplastics Released during Washing and Abrasion of Polyester Textiles.” *Environ Sci Technol* **2022**, *56* (14), 10543–10544. https://doi.org/10.1021/acs.est.1c08880.
(122) Busse, K.; Ebner, I.; Humpf, H.-U.; Ivleva, N.; Kaeppler, A.; Oßmann, B. E.; Schymanski, D. Comment on “Plastic Teabags Release Billions of Microparticles and Nanoparticles into Tea.” *Environ Sci Technol* **2020**, *54* (21), 14134–14135. https://doi.org/10.1021/acs.est.0c03182.
(123) Hernandez, L. M.; Xu, E. G.; Larsson, H. C. E.; Tahara, R.; Maisuria, V. B.; Tufenkji, N. Response to Comment on “Plastic Teabags Release Billions of Microparticles and Nanoparticles into Tea.” *Environ Sci Technol* **2020**, *54* (21), 14136–14137. https://doi.org/10.1021/acs.est.0c06422.
(124) Zangmeister, C. D.; Radney, J. G.; Benkstein, K. D.; Kalanyan, B. Common Single-Use Consumer Plastic Products Release Trillions of Sub-100 Nm Nanoparticles per Liter into Water during Normal Use. *Environ Sci Technol* **2022**, *56* (9), 5448–5455. https://doi.org/10.1021/acs.est.1c06768.
(125) Hernandez, L. M.; Xu, E. G.; Larsson, H. C. E.; Tahara, R.; Maisuria, V. B.; Tufenkji, N. Plastic Teabags Release Billions of Microparticles and Nanoparticles into Tea. *Environ Sci Technol* **2019**, *53* (21), 12300–12310. https://doi.org/10.1021/acs.est.9b02540.

(126) Hernandez, L. M.; Xu, E. G.; Larsson, H. C. E.; Tahara, R.; Maisuria, V. B.; Tufenkji, N. Response to Comment on “Plastic Teabags Release Billions of Microparticles and Nanoparticles into Tea.” *Environ Sci Technol* **2020**, *54* (21), 14136–14137. https://doi.org/10.1021/acs.est.0c06422.
(127) Li, D.; Shi, Y.; Yang, L.; Xiao, L.; Kehoe, D. K.; Gun’ko, Y. K.; Boland, J. J.; Wang, J. J. Microplastic Release from the Degradation of Polypropylene Feeding Bottles during Infant Formula Preparation. *Nat Food* **2020**, *1* (11), 746–754. https://doi.org/10.1038/s43016-020-00171-y.
(128) Su, Y.; Hu, X.; Tang, H.; Lu, K.; Li, H.; Liu, S.; Xing, B.; Ji, R. Steam Disinfection Releases Micro(Nano)Plastics from Silicone-Rubber Baby Teats as Examined by Optical Photothermal Infrared Microspectroscopy. *Nat Nanotechnol* **2022**, *17* (1), 76–85. https://doi.org/10.1038/s41565-021-00998-x.
(129) Yang, T.; Luo, J.; Nowack, B. Characterization of Nanoplastics, Fibrils, and Microplastics Released during Washing and Abrasion of Polyester Textiles. *Environ Sci Technol* **2021**, *55* (23), 15873–15881. https://doi.org/10.1021/acs.est.1c04826.
(130) Yang, T.; Nowack, B. Reply to Comment on “Characterization of Nanoplastics, Fibrils, and Microplastics Released during Washing and Abrasion of Polyester Textiles.” *Environ Sci Technol* **2022**, *56* (14), 10545–10546. https://doi.org/10.1021/acs.est.2c00958.
(131) Yang, T.; Xu, Y.; Liu, G.; Nowack, B. Oligomers Are a Major Fraction of the Submicrometre Particles Released during Washing of Polyester Textiles. *Nature Water* **2024**, *2* (2), 151–160. https://doi.org/10.1038/s44221-023-00191-5.
(132) Dye, B. A.; Thornton-Evans, G.; Li, X.; Iafolla, T. J. *Dental Caries and Tooth Loss in Adults in the United States, 2011–2012 NCHS Data Brief, No 197*; Hyattsville, MD, 2015. https://www.cdc.gov/nchs/products/databriefs/db197.htm (accessed 2023-11-29).

For Table of Contents Only

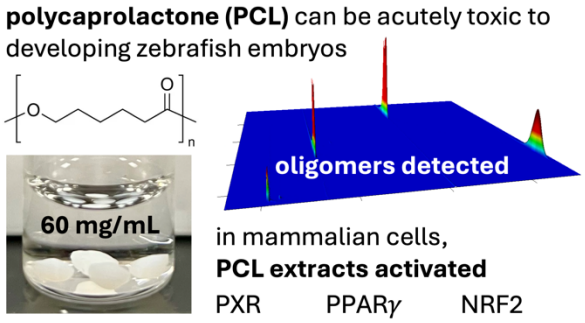

Supporting Information

Moldable plastics (polycaprolactone) can be acutely toxic to developing zebrafish and activate nuclear receptors in mammalian cells

Bryan D. James,[1,2,*] Alexander V. Medvedev,[3] Sergei S. Makarov,[3] Robert K. Nelson,[1] Christopher M. Reddy,[1] Mark E. Hahn[2]

[1]Department of Marine Chemistry and Geochemistry, Woods Hole Oceanographic Institution, Woods Hole, MA, USA 02543

[2]Department of Biology, Woods Hole Oceanographic Institution, Woods Hole, MA, USA 02543

[3]Attagene, Research Triangle Park, Morrisville, NC, USA 27709

*Corresponding author; Email: bjames@whoi.edu

EXTENDED MATERIALS AND METHODS

GC×GC-FID Method

GC×GC-FID chromatographic analyses were performed on a Leco instrument system consisting of an Agilent 7890A GC configured with a split/splitless auto-injector (7683B series) and a dual stage cryogenic modulator (Leco, Saint Joseph, Michigan). Samples were injected in splitless mode. The cold jet gas was dry N_2 chilled with liquid N_2. The hot jet temperature offset was 5 °C above the temperature of the main GC oven and the inlet temperature was isothermal at 310 °C. Two capillary GC columns were utilized in this GC×GC experiment. The first-dimension column was a Restek Rxi-1ms, (60-m length, 0.25 mm I.D., 0.25 µm df) and second-dimension separations were performed on a 50% phenyl polysilphenylene-siloxane column (SGE BPX50, 1.2-m length, 0.10 mm I.D., 0.1 µm df). The temperature program of the main oven was held isothermal at 65 °C (12.5 min) and was then ramped from 65 to 340 °C at 1.25 °C min^{-1}. The second-dimension oven was isothermal at 70 °C (12.5 min) and then ramped from 70 to 345 °C at 1.25 °C. The hot jet pulse width was 1.0 seconds, the modulation period was 6.5 seconds with a 2.25 second cooling period between stages, GC×GC-FID data was sampled at an acquisition rate of 100 data points per second. The carrier gas was hydrogen (H_2) at a flow rate of 1 mL min^{-1}.

GC×GC-HRT Method

GC×GC-HRT chromatographic analysis was performed on a Leco Pegasus GC×GC-HRT 4D system consisting of an Agilent 7890B GC configured with a Leco LPAL3 split/splitless auto-injector system and a dual stage cryogenic modulator (Leco, Saint Joseph, Michigan). Samples were injected in splitless mode. The cold jet gas was dry N_2 chilled with liquid N_2. The hot jet temperature offset was 25 °C above the temperature of the main GC oven and the inlet temperature was isothermal at 310 °C. Two capillary GC columns were utilized in this GC×GC experiment. The first-dimension column was a Restek Rxi-1ms, (60-m length, 0.25 mm I.D., 0.25 µm df) and second-dimension separations were performed on a 50% phenyl polysilphenylene-siloxane column (SGE BPX50, 1.2-m length, 0.10 mm I.D., 0.1 µm df). The temperature program of the main oven was held isothermal at 75 °C (12.5 min) and was then ramped from 75 to 315 °C at 1.25 °C min^{-1}. The second-dimension oven was isothermal at 88 °C (12.5 min) and then ramped from 88 to 328 °C at 1.25 °C. The hot jet pulse width was 2.4 seconds, the modulation period was 8.00 seconds with a 1.6 second cooling period between stages, GC×GC-HRT data was sampled at an acquisition rate of 194.44 spectra per second in the mass range of 40 to 500 atomic mass units (amu). The carrier gas was helium (He) at a flow rate of 1 mL min-1. HR-TOF data was sampled at an acquisition rate of 200 spectra per second (actual data collection rate was 194.44 spectra per second) in the mass range of 40 to 500 amu. The ionization method was electron ionization (EI) with an electron energy of -70 Volts and the extraction frequency was 1.75 kHz.

GC×GC QA/QC

National Institute of Standards and Technology (NIST) standard reference material SRM-1582 (Petroleum Crude Oil) was used to calibrate and validate the GC×GC instruments. GC×GC performance was monitored on all instruments using SRM-1582. SRM-1582 samples were routinely interspersed with analytical samples and to monitor a suite of biomarker ratios to confirm that the instruments were stable and operating as expected.

GC×GC-HRT Calibration

GC×GC-HRT mass spectra were calibrated using a continuous flow of perfluorotributylamine (PFTBA) introduced by opening a valve into the EI source in the GC×GC-HRT instrument. GC×GC-HRT data collected throughout each EI run is calibrated with respect to the molecular ion (+1 charge state) of eight perfluorinated compounds (CF_3, C_2F_4, C_2F_5, C_3F_5, C_4F_9, $C_5F_{10}N$, $C_8F_{16}N$, and $C_9F_{20}N$). The mass values for singly charged ions in the mass range of 40-650 amu, with a relative abundance at least ten times the signal to noise ratio of the base plane were acquired and stored. Additional GC×GC-HRT data processing was performed using a petroleomics mass spectral data analysis application for LECO's ChromaTOF software.

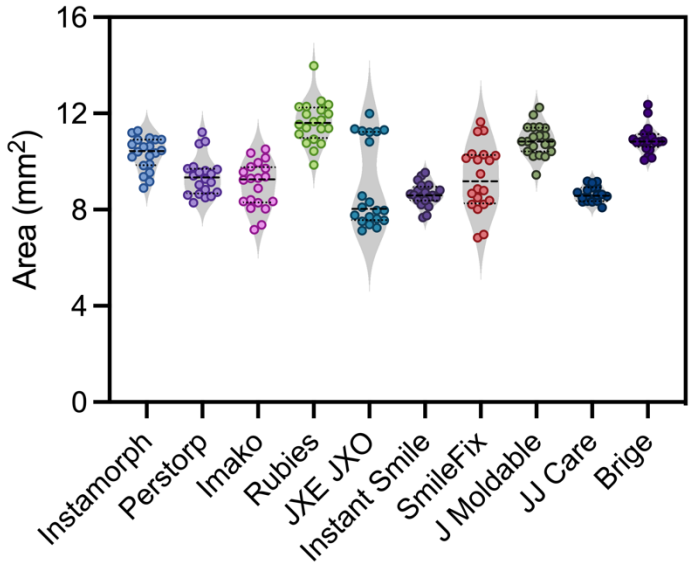

Figure S1. Projected area of the moldable plastic pellets. Data points represent values for individual pellets. n = 18-20. Dashed lines represent the median, 25th quartile, and 75th quartile.

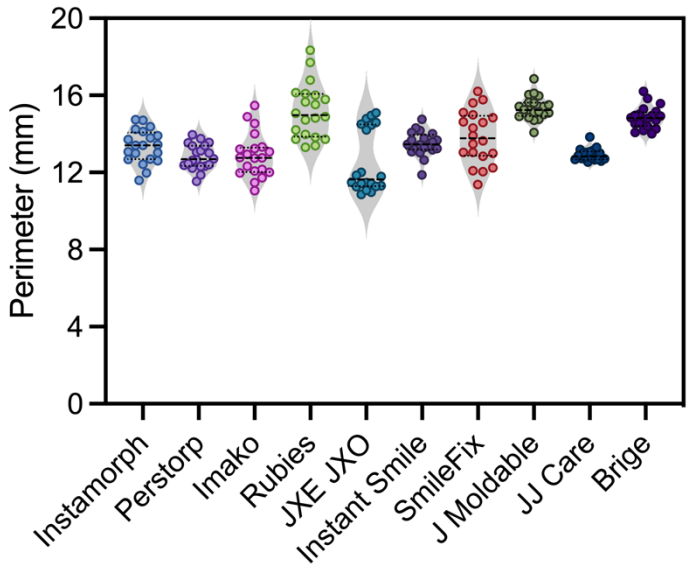

Figure S2. Projected perimeter of the moldable plastic pellets. Data points represent values for individual pellets. n = 18-20. Dashed lines represent the median, 25th quartile, and 75th quartile.

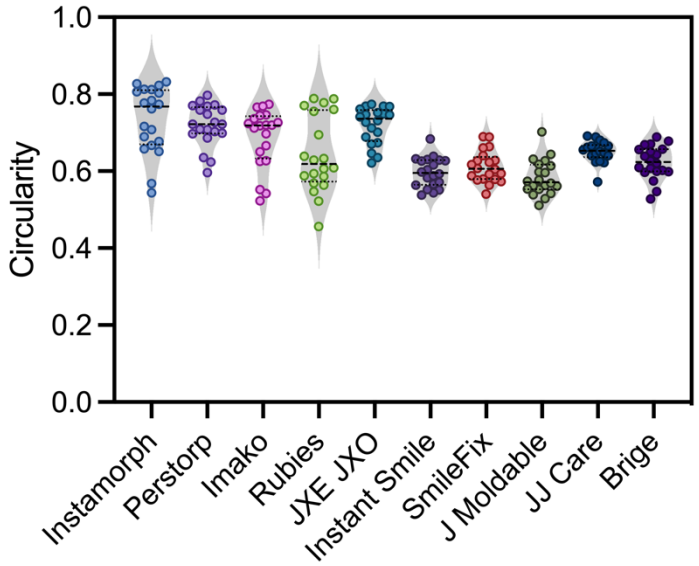

Figure S3. Circularity of the moldable plastic pellets. Data points represent values for individual pellets. n = 18-20. Dashed lines represent the median, 25th quartile, and 75th quartile.

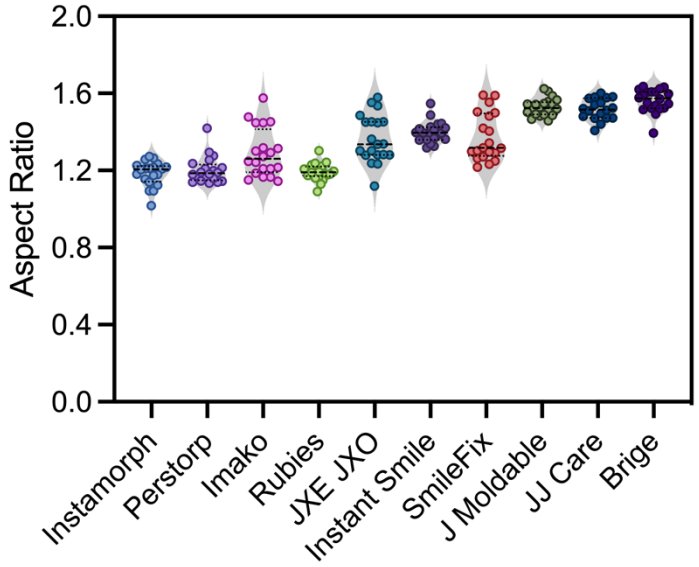

Figure S4. Aspect ratio of the moldable plastic pellets. Data points represent values for individual pellets. n = 18-20. Dashed lines represent the median, 25th quartile, and 75th quartile.

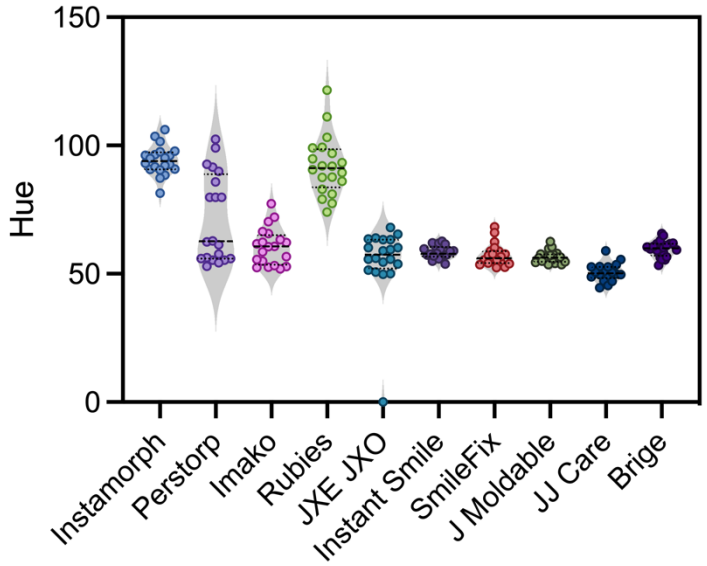

Figure S5. Average hue of the moldable plastic pellets. Data points represent individual pellets for each product. n = 18-20. Dashed lines represent the median, 25th quartile, and 75th quartile.

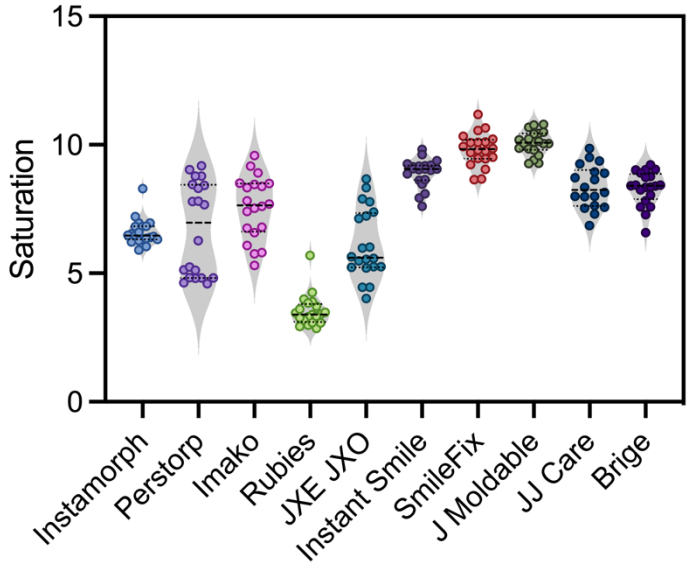

Figure S6. Average saturation of the moldable plastic pellets. Data points represent values for individual pellets. n = 18-20. Dashed lines represent the median, 25th quartile, and 75th quartile.

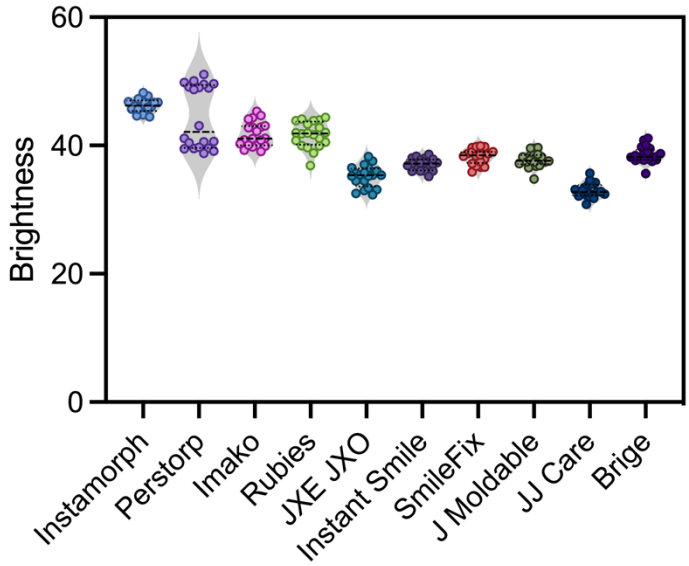

Figure S7. Average brightness of the moldable plastic pellets. Data points represent values for individual pellets. n = 18-20. Dashed lines represent the median, 25th quartile, and 75th quartile.

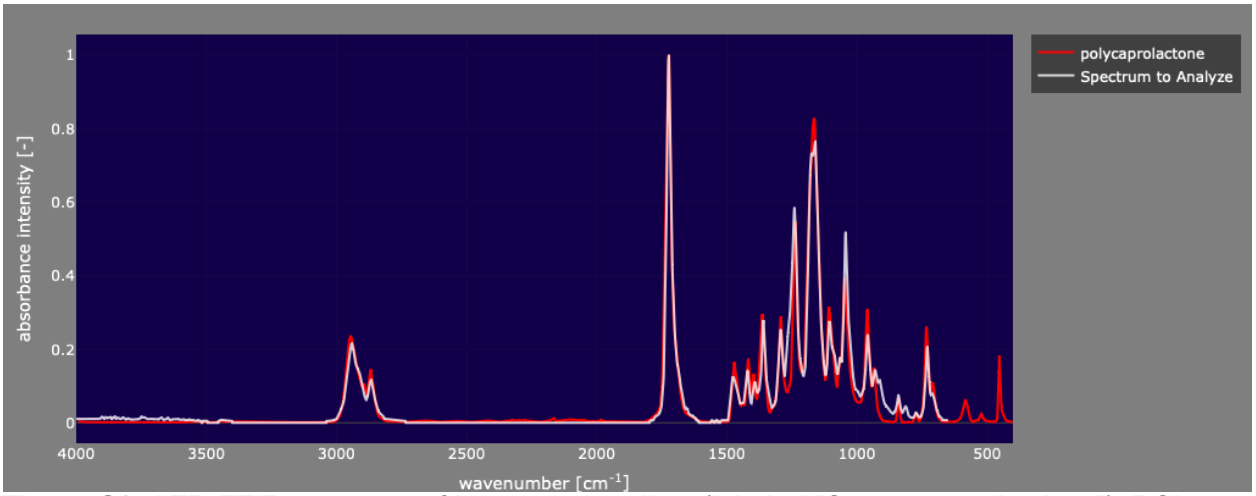

Figure S8. ATR-FTIR spectrum of Instamorph pellets (labeled "Spectrum to Analyze"). PCL reference is in red. Figure exported from Open Specy. Pearson's r = 0.97.

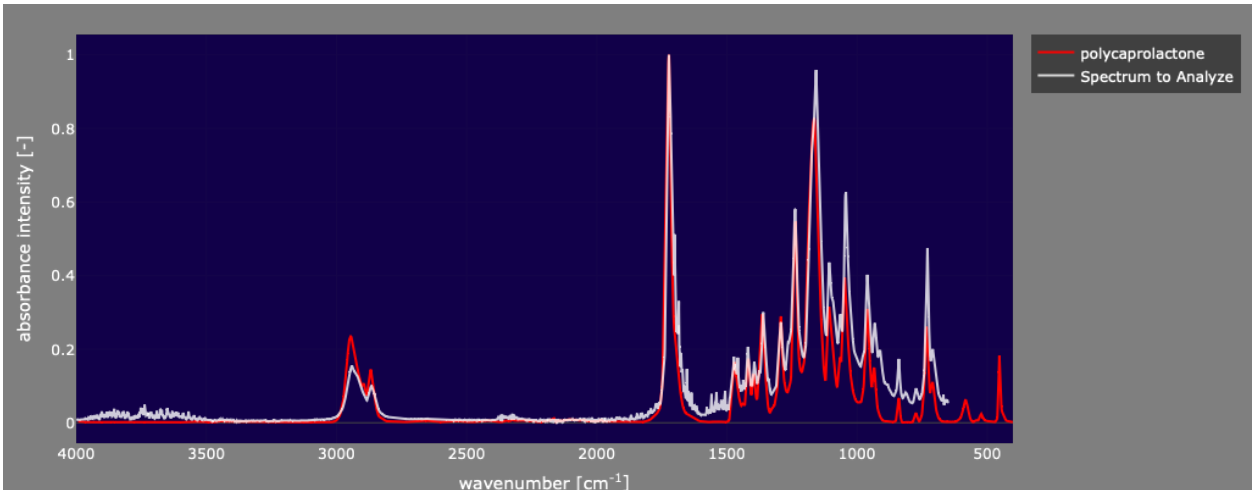

Figure S9. ATR-FTIR spectrum of Perstorp pellets (labeled "Spectrum to Analyze"). PCL reference is in red. Figure exported from Open Specy.[1] Pearson's r = 0.96.

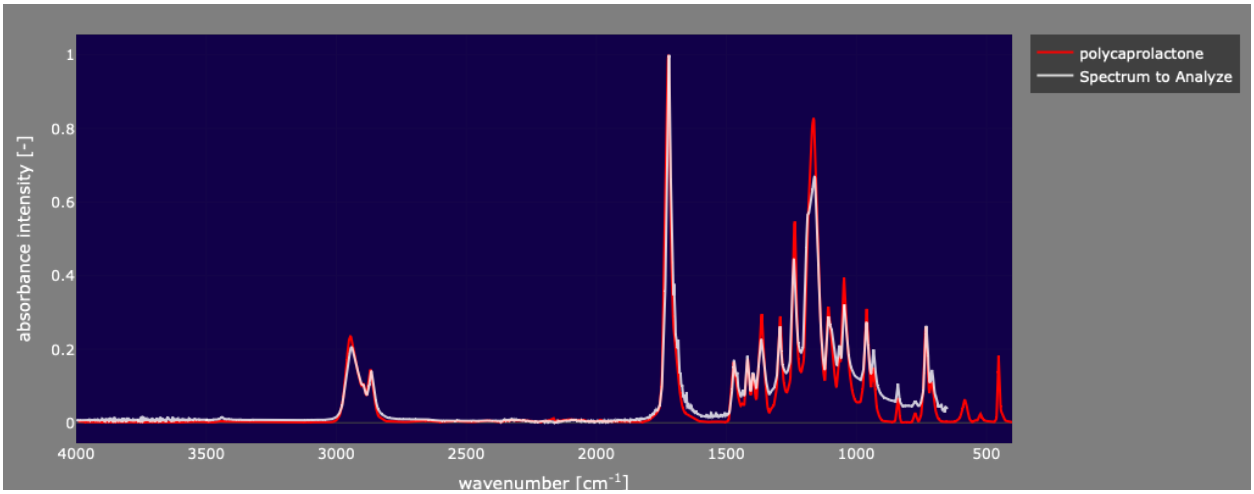

Figure S10. ATR-FTIR spectrum of Polly Plastic sheet (labeled "Spectrum to Analyze"). PCL reference is in red. Figure exported from Open Specy.[1] Pearson's r = 0.97.

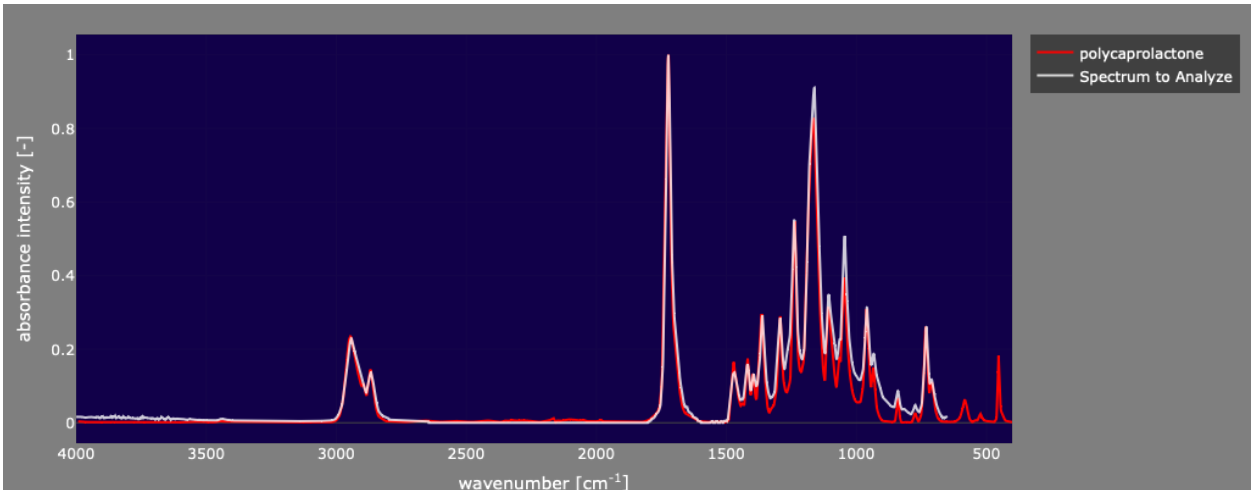

Figure S11. ATR-FTIR spectrum of Imako pellets (labeled "Spectrum to Analyze"). PCL reference is in red. Figure exported from Open Specy.[1] Pearson's r = 0.98.

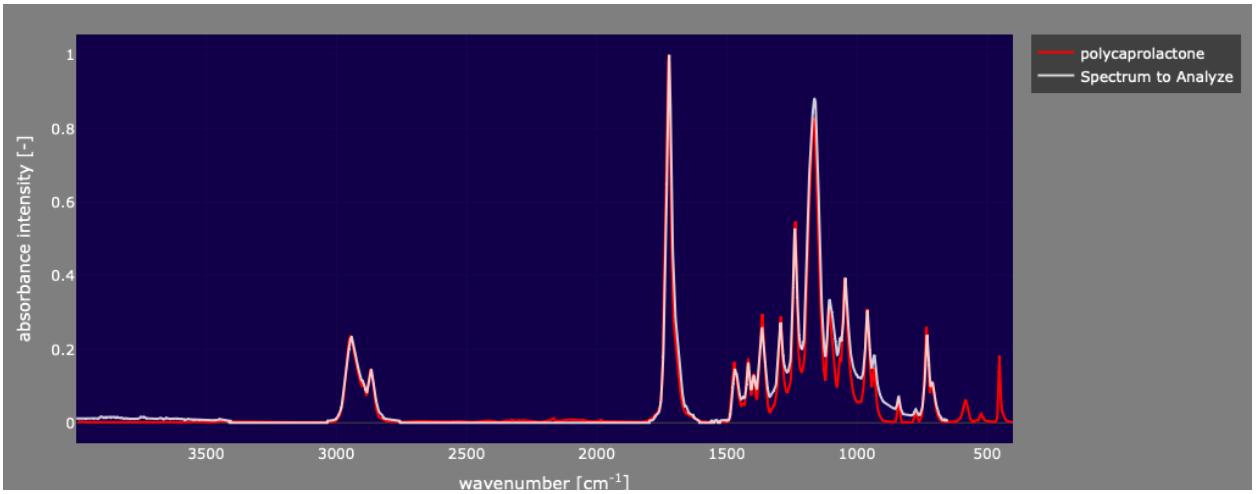

Figure S12. ATR-FTIR spectrum of Rubies pellets (labeled "Spectrum to Analyze"). PCL reference is in red. Figure exported from Open Specy.[1] Pearson's r = 0.99.

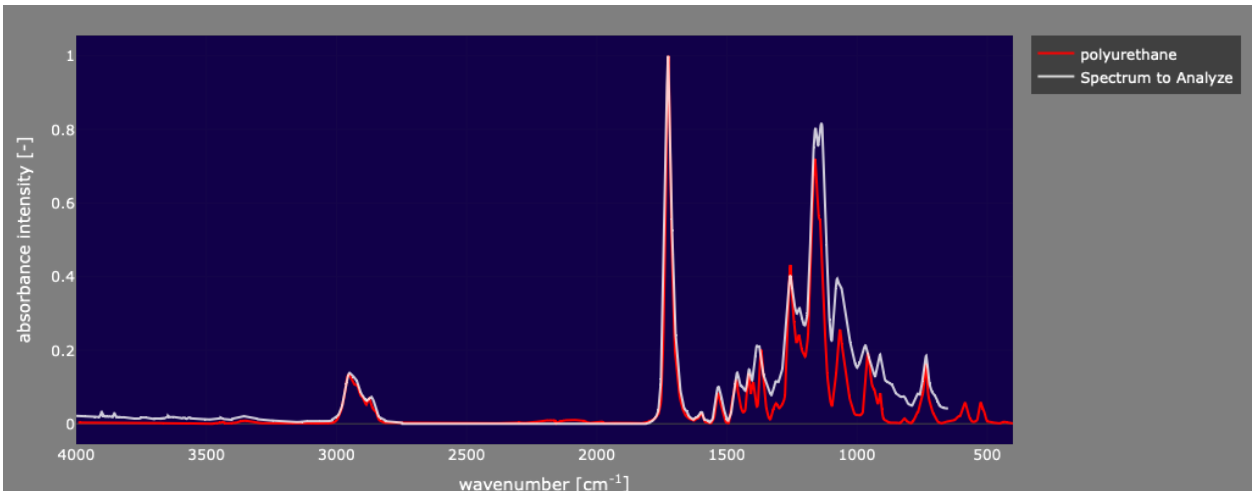

Figure S13. ATR-FTIR spectrum of JXE JXO pellets (labeled "Spectrum to Analyze"). TPU reference in red. Figure exported from Open Specy.[1] Pearson's r = 0.95.

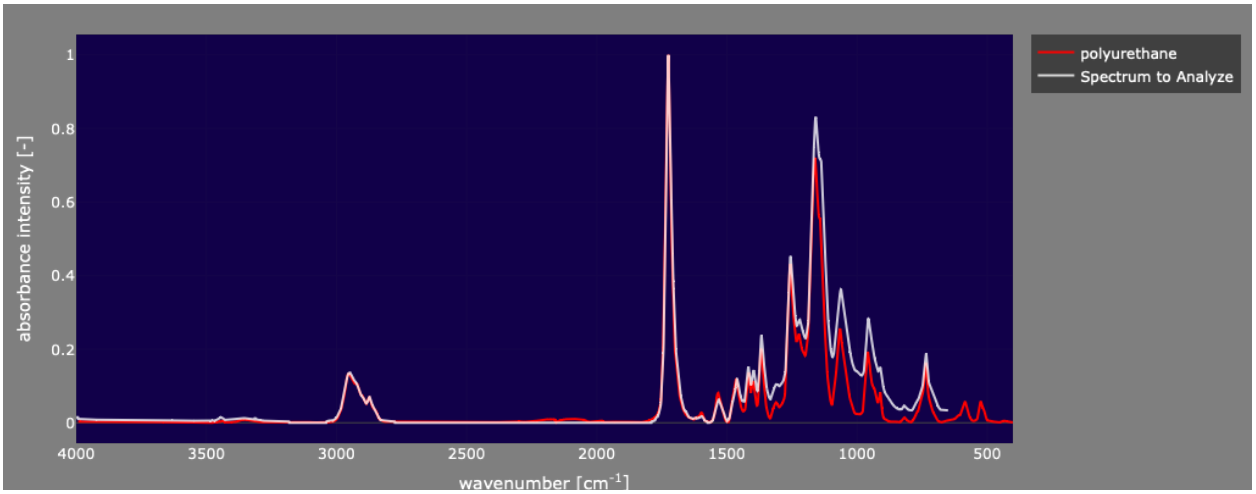

Figure S14. ATR-FTIR spectrum of uxcell 3D pen filament (labeled "Spectrum to Analyze"). TPU reference is in red. Figure exported from Open Specy.[1] Pearson's r = 0.96.

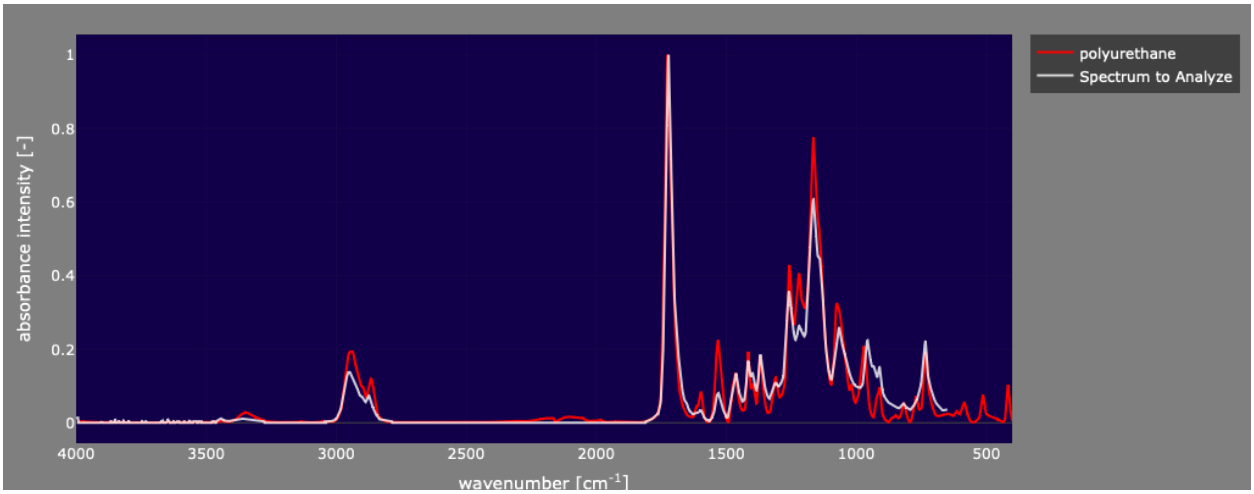

Figure S15. ATR-FTIR spectrum of InstantSmile pellets (labeled "Spectrum to Analyze"). TPU reference is in red. Figure exported from Open Specy.[1] Pearson's r = 0.96.

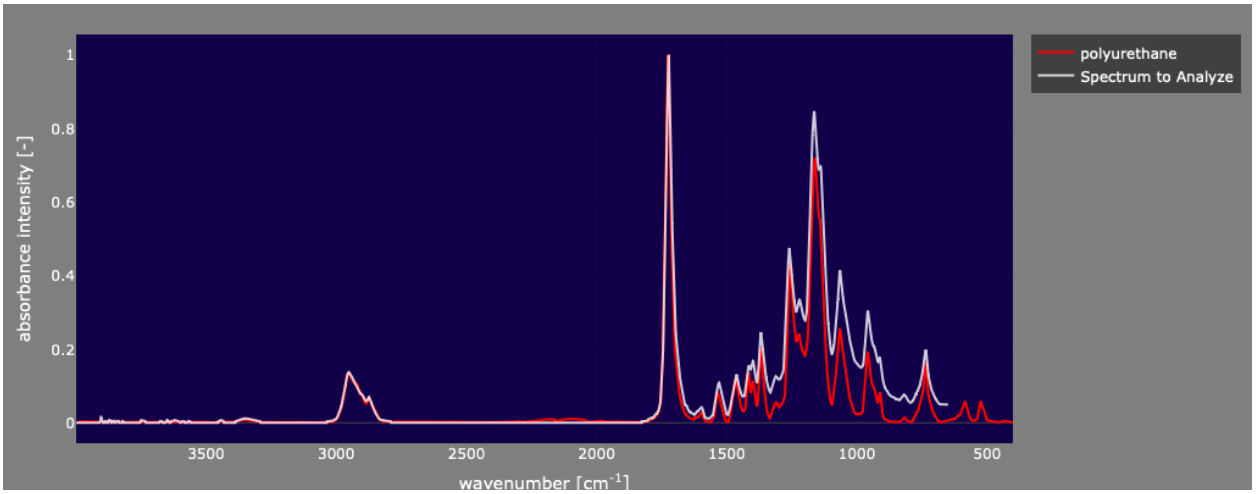

Figure S16. ATR-FTIR spectrum of SmileFix pellets (labeled "Spectrum to Analyze"). TPU reference is in red. Figure exported from Open Specy.[1] Pearson's r = 0.96.

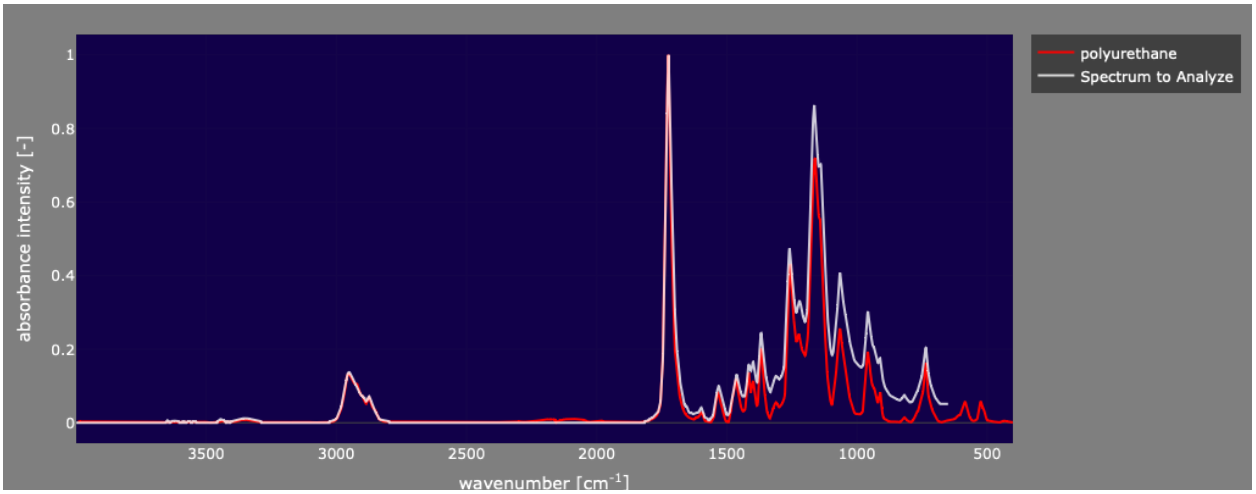

Figure S17. ATR-FTIR spectrum of JJ Care pellets (labeled "Spectrum to Analyze"). TPU reference is in red. Figure exported from Open Specy.[1] Pearson's r = 0.96.

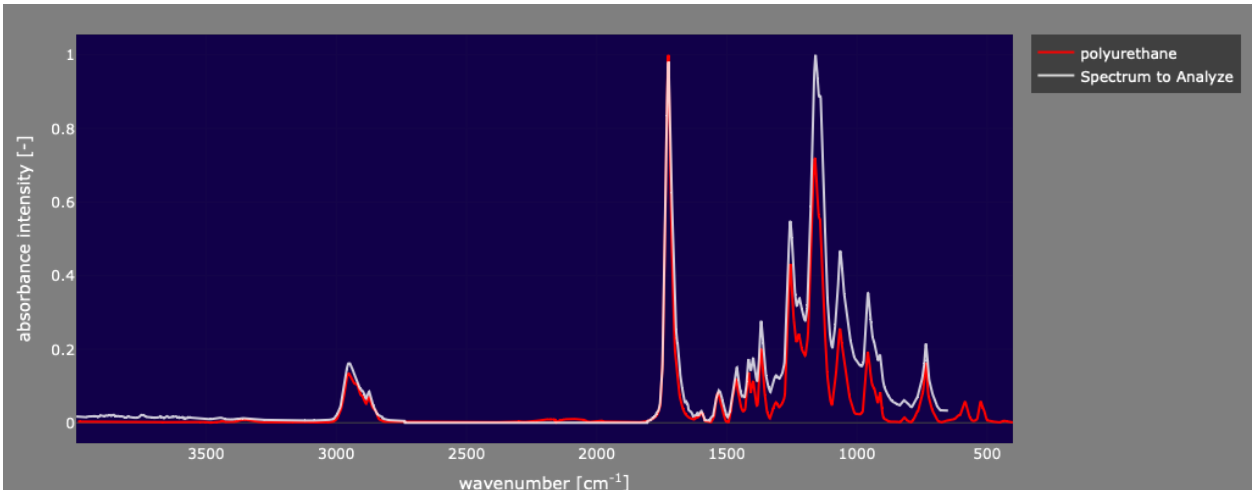

Figure S18. ATR-FTIR spectrum of Brige pellets (labeled "Spectrum to Analyze"). TPU reference is in red. Figure exported from Open Specy.[1] Pearson's r = 0.96.

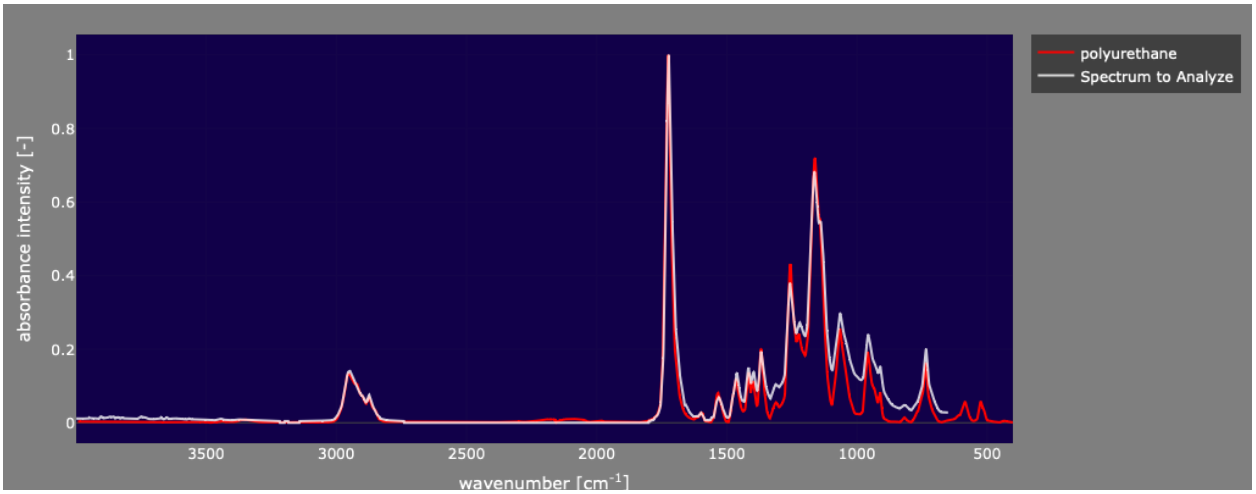

Figure S19. ATR-FTIR spectrum of J Moldable pellets (labeled "Spectrum to Analyze"). TPU reference is in red. Figure exported from Open Specy.[1] Pearson's r = 0.97.

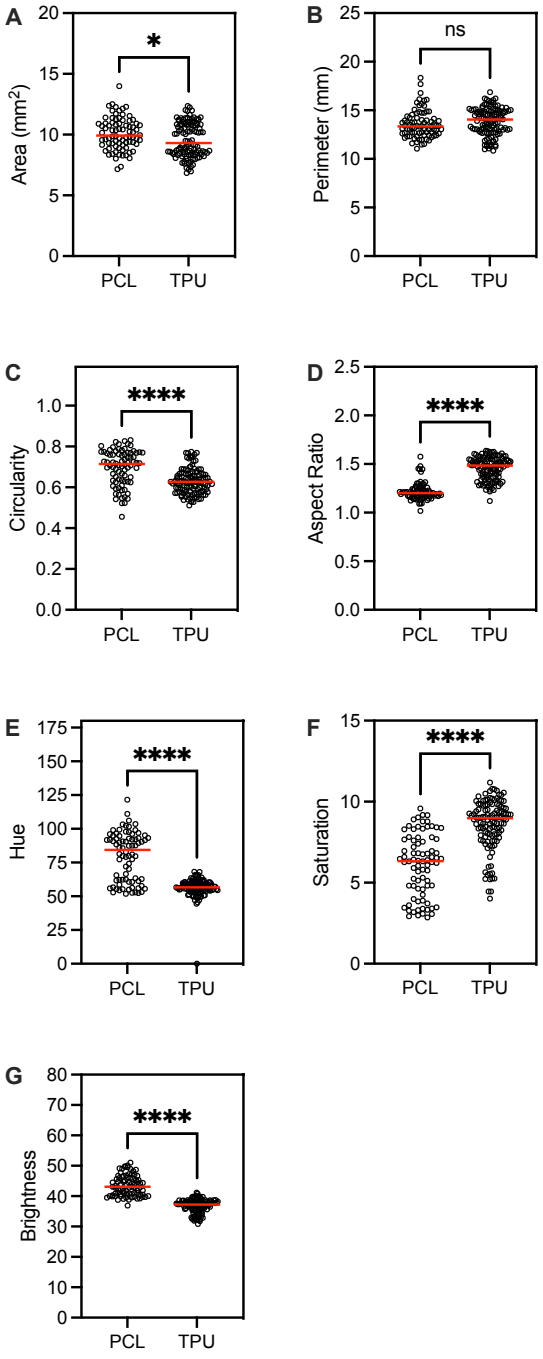

Figure S20. (**A**) Projected area, (**B**) projected perimeter, (**C**) circularity, (**D**) aspect ratio, (**E**) hue, (**F**) saturation, and (**G**) brightness of the moldable plastic pellets. Data points represent values for individual pellets. n = 80 for PCL and 118 for TPU. Lines indicate median value. Statistical significance was determined for A-D by an unpaired t test with Welch's correction and for E-G by a Mann Whitney test. * indicates *p* value < 0.05. **** indicates *p* value < 0.0001. ns indicates *p* value > 0.05.

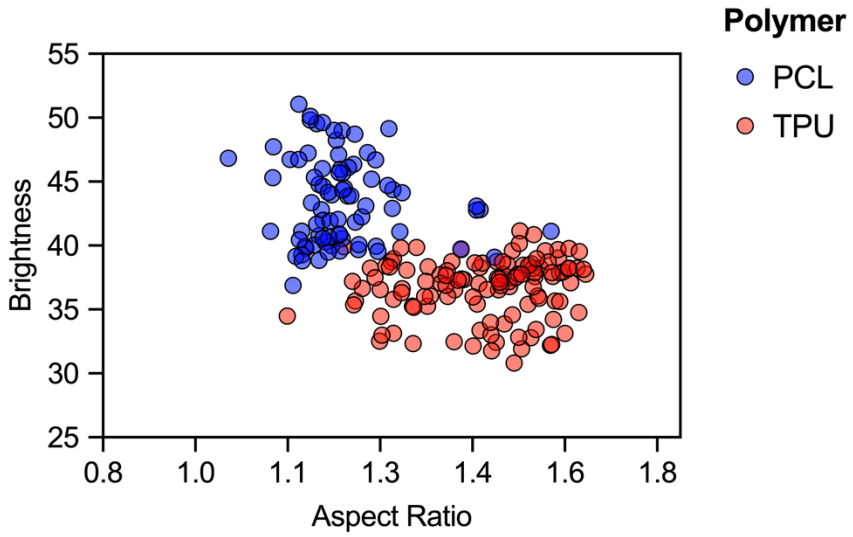

Figure S21. Clustering of polymer type for the moldable plastic pellets. Data points represent values for individual pellets. n = 80 for PCL and 118 for TPU.

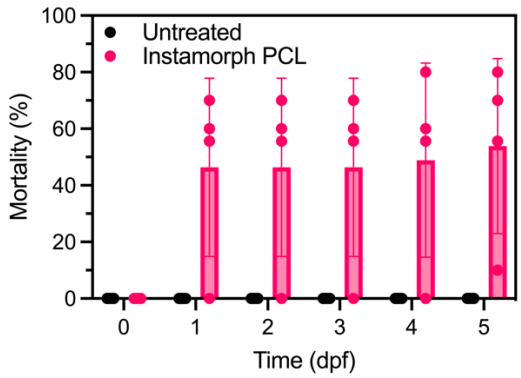

Figure S22. Mortality of untreated zebrafish embryos and those continuously exposed to 2 pellets/mL of consumer-grade PCL. Each treatment was measured in quadruplicate with 10 embryos per replicate.

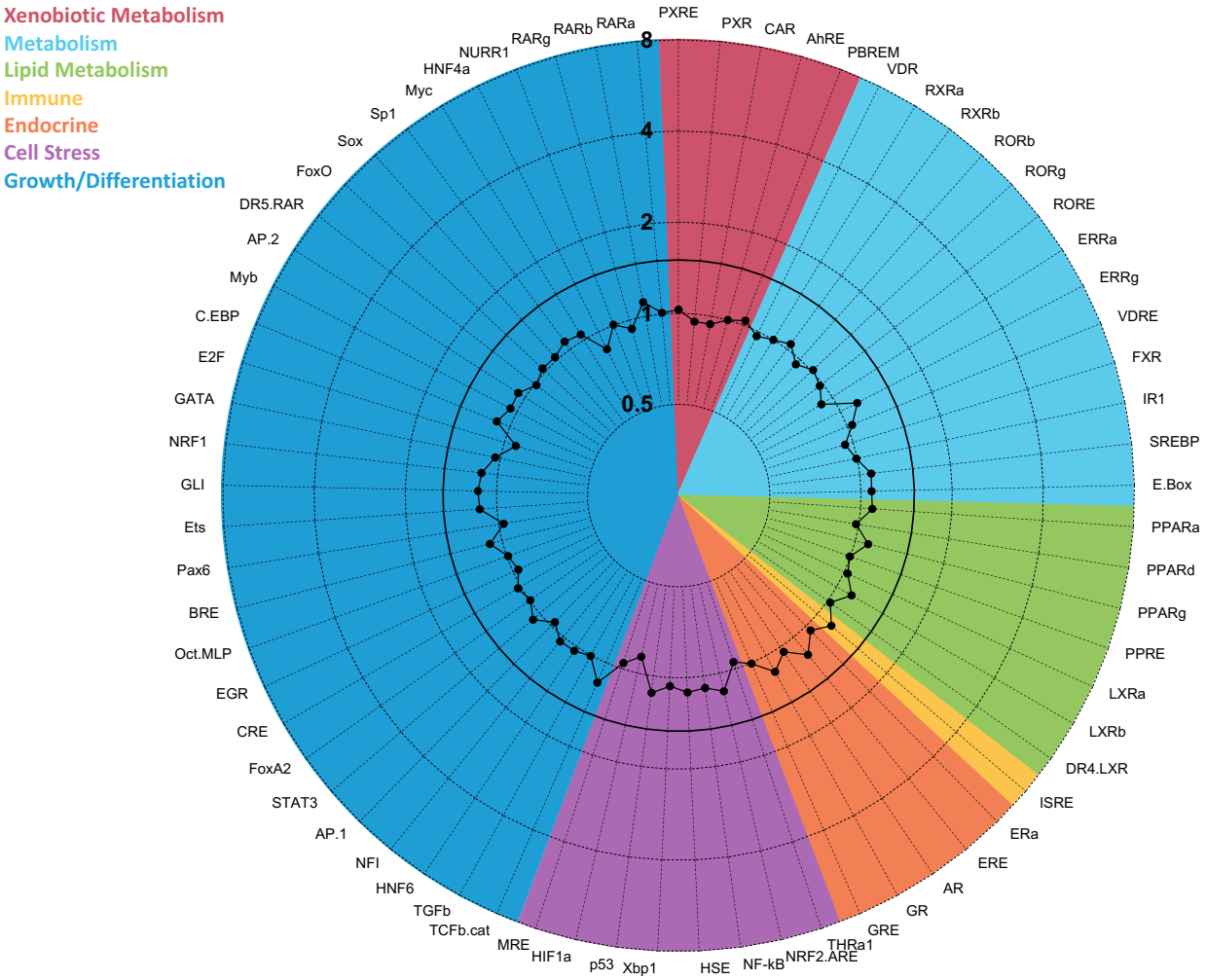

Figure S23. TF-Factorial and NR-Factorial endpoints (solid circles) for extraction blank did not exceed the induction threshold of 1.5 (solid circle). Fold activation of all 45 human transcription factor response elements and 24 nuclear receptors tested for activity in the bioassays are included in **Table S3**.

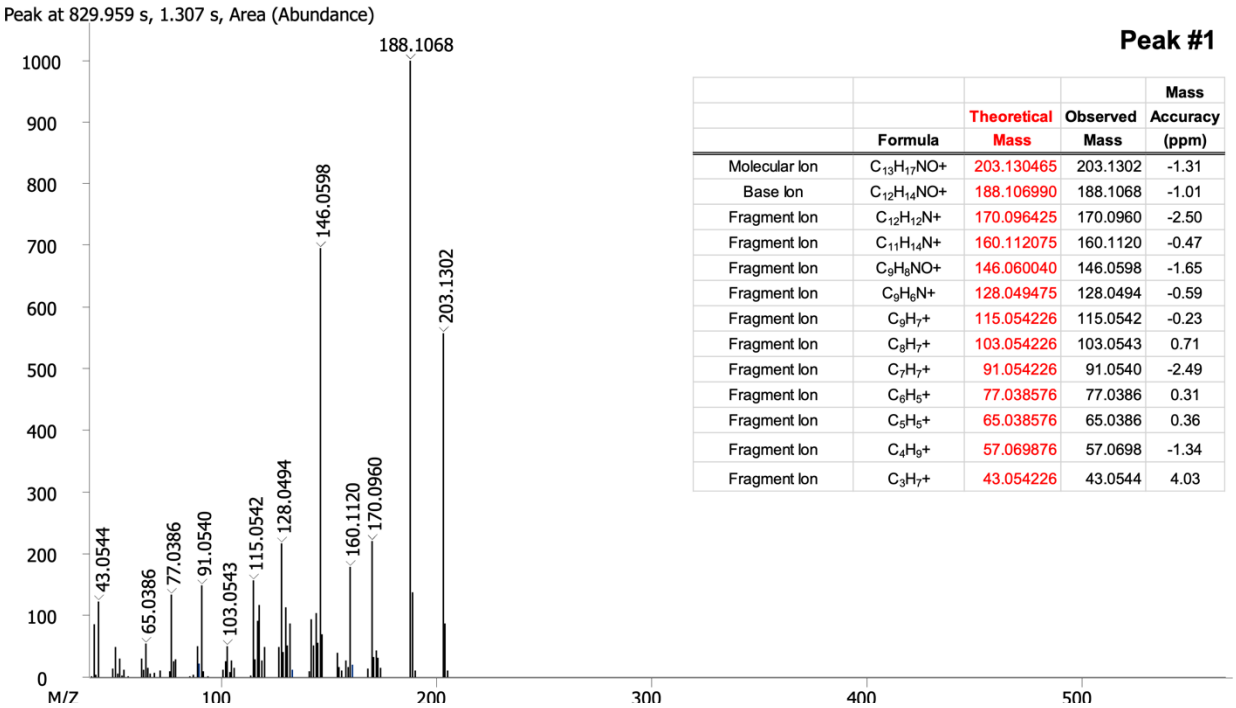

Peak #1

	Formula	Theoretical Mass	Observed Mass	Mass Accuracy (ppm)
Molecular Ion	$C_{13}H_{17}NO+$	203.130465	203.1302	-1.31
Base Ion	$C_{12}H_{14}NO+$	188.106990	188.1068	-1.01
Fragment Ion	$C_{12}H_{12}N+$	170.096425	170.0960	-2.50
Fragment Ion	$C_{11}H_{14}N+$	160.112075	160.1120	-0.47
Fragment Ion	C_9H_8NO+	146.060040	146.0598	-1.65
Fragment Ion	C_9H_6N+	128.049475	128.0494	-0.59
Fragment Ion	C_9H_7+	115.054226	115.0542	-0.23
Fragment Ion	C_8H_7+	103.054226	103.0543	0.71
Fragment Ion	C_7H_7+	91.054226	91.0540	-2.49
Fragment Ion	C_6H_5+	77.038576	77.0386	0.31
Fragment Ion	C_5H_5+	65.038576	65.0386	0.36
Fragment Ion	C_4H_9+	57.069876	57.0698	-1.34
Fragment Ion	C_3H_7+	43.054226	43.0544	4.03

Figure S24. Mass spectrum of peak 1. Refer to **Figure 4** for chromatographic positioning.

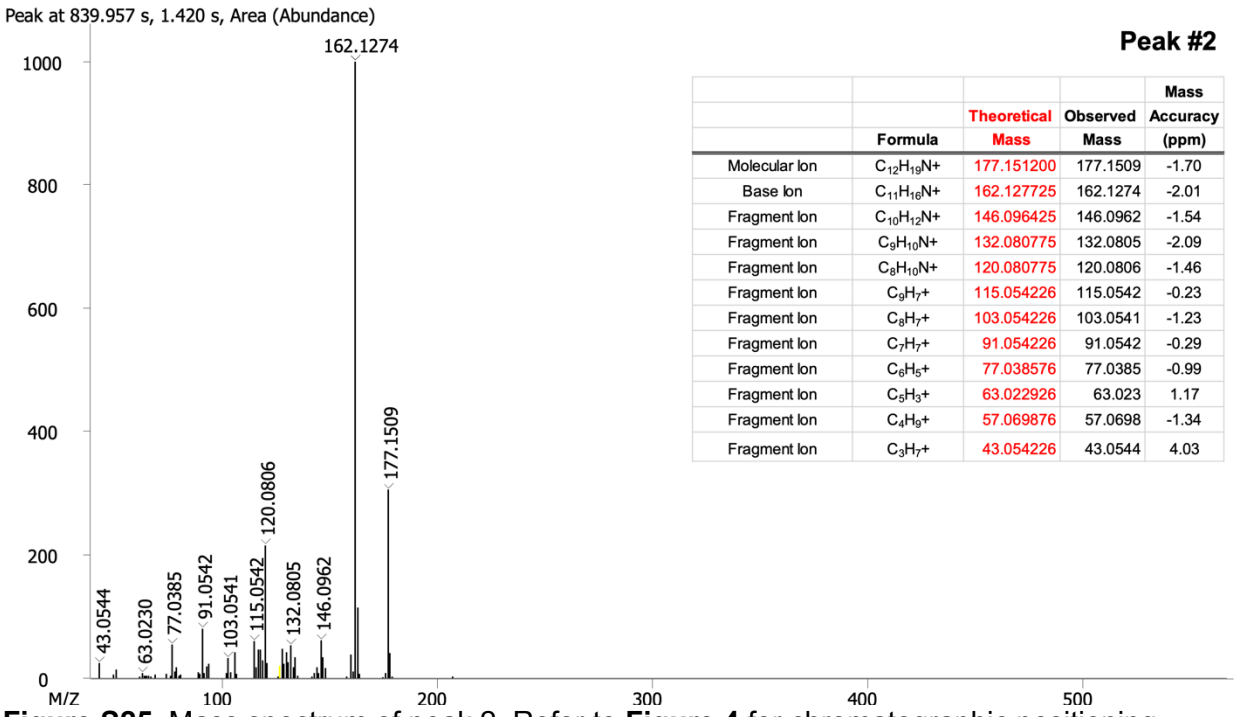

Peak #2

	Formula	Theoretical Mass	Observed Mass	Mass Accuracy (ppm)
Molecular Ion	$C_{12}H_{19}N+$	177.151200	177.1509	-1.70
Base Ion	$C_{11}H_{16}N+$	162.127725	162.1274	-2.01
Fragment Ion	$C_{10}H_{12}N+$	146.096425	146.0962	-1.54
Fragment Ion	$C_9H_{10}N+$	132.080775	132.0805	-2.09
Fragment Ion	$C_8H_{10}N+$	120.080775	120.0806	-1.46
Fragment Ion	C_9H_7+	115.054226	115.0542	-0.23
Fragment Ion	C_8H_7+	103.054226	103.0541	-1.23
Fragment Ion	C_7H_7+	91.054226	91.0542	-0.29
Fragment Ion	C_6H_5+	77.038576	77.0385	-0.99
Fragment Ion	C_5H_3+	63.022926	63.023	1.17
Fragment Ion	C_4H_9+	57.069876	57.0698	-1.34
Fragment Ion	C_3H_7+	43.054226	43.0544	4.03

Figure S25. Mass spectrum of peak 2. Refer to **Figure 4** for chromatographic positioning.

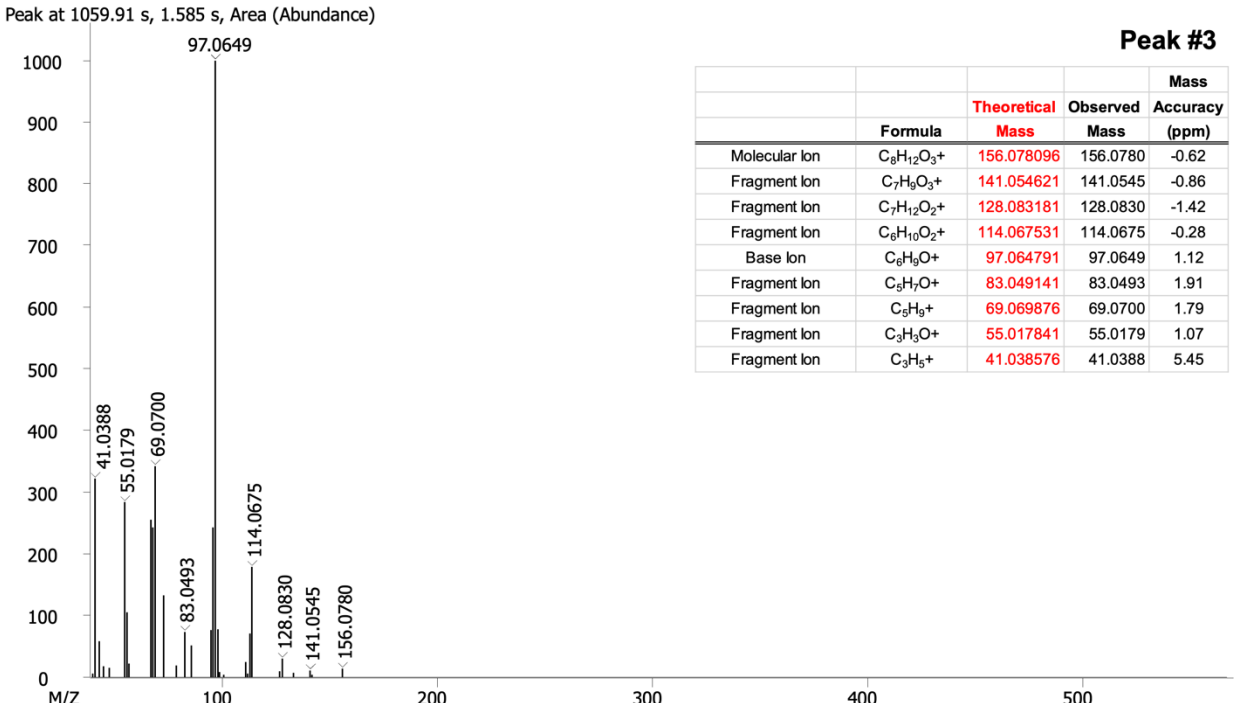

Peak #3

	Formula	Theoretical Mass	Observed Mass	Mass Accuracy (ppm)
Molecular Ion	$C_8H_{12}O_3$+	156.078096	156.0780	-0.62
Fragment Ion	$C_7H_9O_3$+	141.054621	141.0545	-0.86
Fragment Ion	$C_7H_{12}O_2$+	128.083181	128.0830	-1.42
Fragment Ion	$C_6H_{10}O_2$+	114.067531	114.0675	-0.28
Base Ion	C_6H_9O+	97.064791	97.0649	1.12
Fragment Ion	C_5H_7O+	83.049141	83.0493	1.91
Fragment Ion	C_5H_9+	69.069876	69.0700	1.79
Fragment Ion	C_3H_3O+	55.017841	55.0179	1.07
Fragment Ion	C_3H_5+	41.038576	41.0388	5.45

Figure S26. Mass spectrum of peak 3. Refer to **Figure 4** for chromatographic positioning.

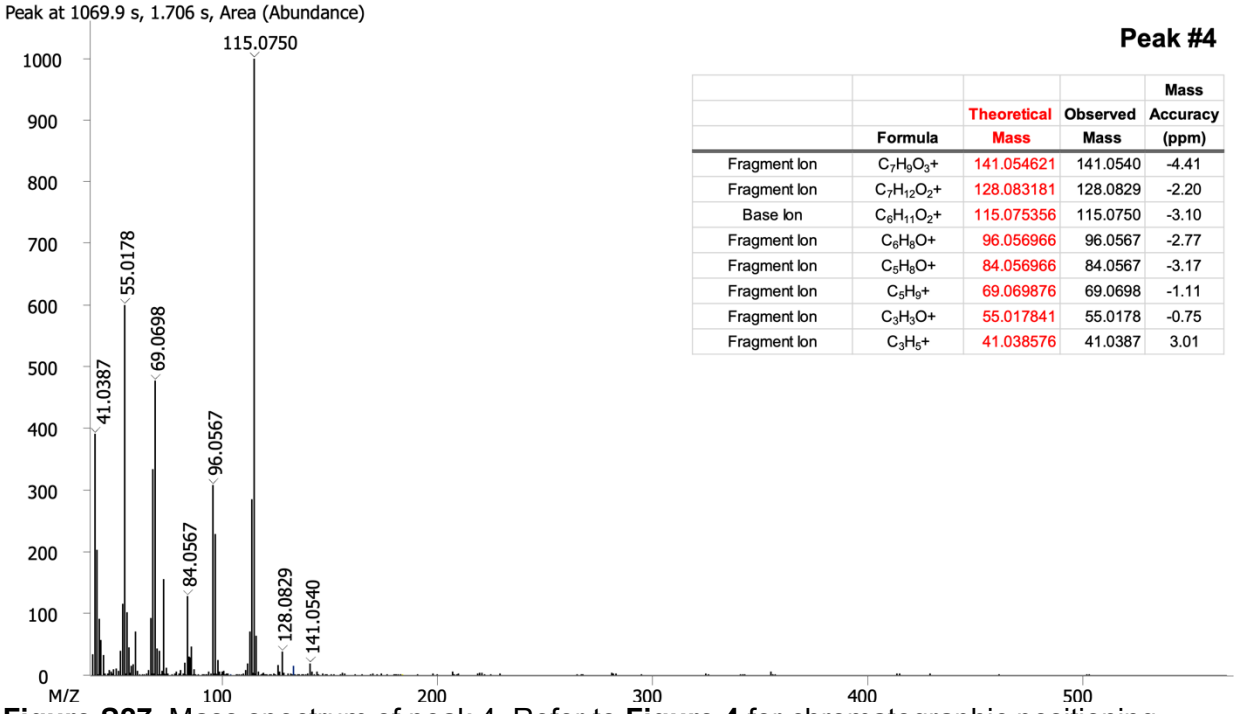

Peak #4

	Formula	Theoretical Mass	Observed Mass	Mass Accuracy (ppm)
Fragment Ion	$C_7H_9O_3$+	141.054621	141.0540	-4.41
Fragment Ion	$C_7H_{12}O_2$+	128.083181	128.0829	-2.20
Base Ion	$C_6H_{11}O_2$+	115.075356	115.0750	-3.10
Fragment Ion	C_6H_8O+	96.056966	96.0567	-2.77
Fragment Ion	C_5H_8O+	84.056966	84.0567	-3.17
Fragment Ion	C_5H_9+	69.069876	69.0698	-1.11
Fragment Ion	C_3H_3O+	55.017841	55.0178	-0.75
Fragment Ion	C_3H_5+	41.038576	41.0387	3.01

Figure S27. Mass spectrum of peak 4. Refer to **Figure 4** for chromatographic positioning.

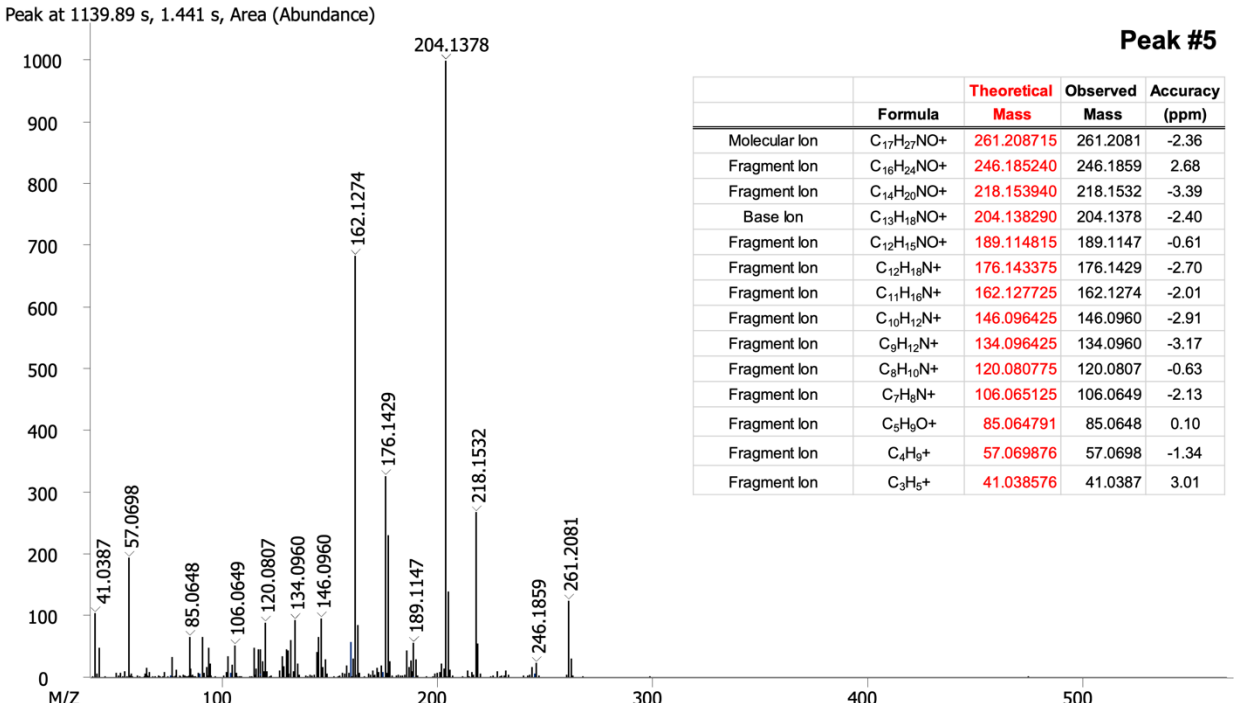

	Formula	Theoretical Mass	Observed Mass	Accuracy (ppm)
Molecular Ion	$C_{17}H_{27}NO+$	261.208715	261.2081	-2.36
Fragment Ion	$C_{16}H_{24}NO+$	246.185240	246.1859	2.68
Fragment Ion	$C_{14}H_{20}NO+$	218.153940	218.1532	-3.39
Base Ion	$C_{13}H_{18}NO+$	204.138290	204.1378	-2.40
Fragment Ion	$C_{12}H_{15}NO+$	189.114815	189.1147	-0.61
Fragment Ion	$C_{12}H_{18}N+$	176.143375	176.1429	-2.70
Fragment Ion	$C_{11}H_{16}N+$	162.127725	162.1274	-2.01
Fragment Ion	$C_{10}H_{12}N+$	146.096425	146.0960	-2.91
Fragment Ion	$C_{9}H_{12}N+$	134.096425	134.0960	-3.17
Fragment Ion	$C_{8}H_{10}N+$	120.080775	120.0807	-0.63
Fragment Ion	$C_{7}H_{8}N+$	106.065125	106.0649	-2.13
Fragment Ion	$C_{5}H_{9}O+$	85.064791	85.0648	0.10
Fragment Ion	$C_{4}H_{9}+$	57.069876	57.0698	-1.34
Fragment Ion	$C_{3}H_{5}+$	41.038576	41.0387	3.01

Figure S28. Mass spectrum of peak 5. Refer to **Figure 4** for chromatographic positioning.

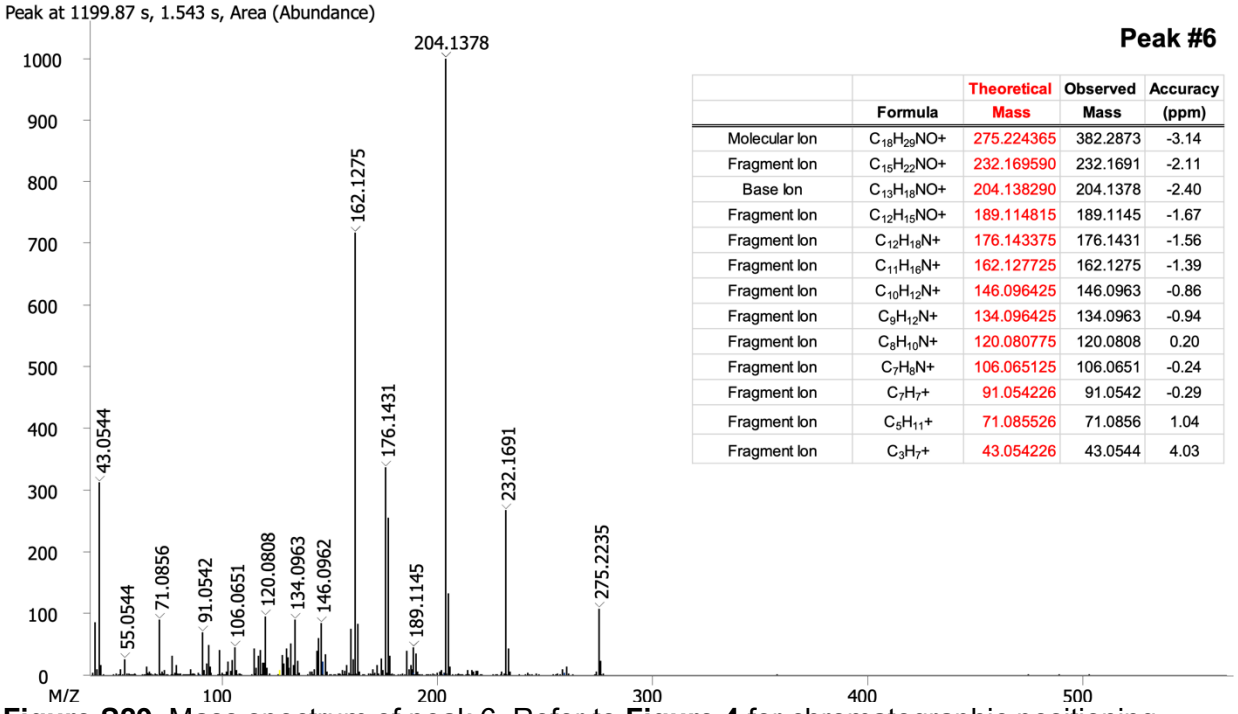

	Formula	Theoretical Mass	Observed Mass	Accuracy (ppm)
Molecular Ion	$C_{18}H_{29}NO+$	275.224365	382.2873	-3.14
Fragment Ion	$C_{15}H_{22}NO+$	232.169590	232.1691	-2.11
Base Ion	$C_{13}H_{18}NO+$	204.138290	204.1378	-2.40
Fragment Ion	$C_{12}H_{15}NO+$	189.114815	189.1145	-1.67
Fragment Ion	$C_{12}H_{18}N+$	176.143375	176.1431	-1.56
Fragment Ion	$C_{11}H_{16}N+$	162.127725	162.1275	-1.39
Fragment Ion	$C_{10}H_{12}N+$	146.096425	146.0963	-0.86
Fragment Ion	$C_{9}H_{12}N+$	134.096425	134.0963	-0.94
Fragment Ion	$C_{8}H_{10}N+$	120.080775	120.0808	0.20
Fragment Ion	$C_{7}H_{8}N+$	106.065125	106.0651	-0.24
Fragment Ion	$C_{7}H_{7}+$	91.054226	91.0542	-0.29
Fragment Ion	$C_{5}H_{11}+$	71.085526	71.0856	1.04
Fragment Ion	$C_{3}H_{7}+$	43.054226	43.0544	4.03

Figure S29. Mass spectrum of peak 6. Refer to **Figure 4** for chromatographic positioning.

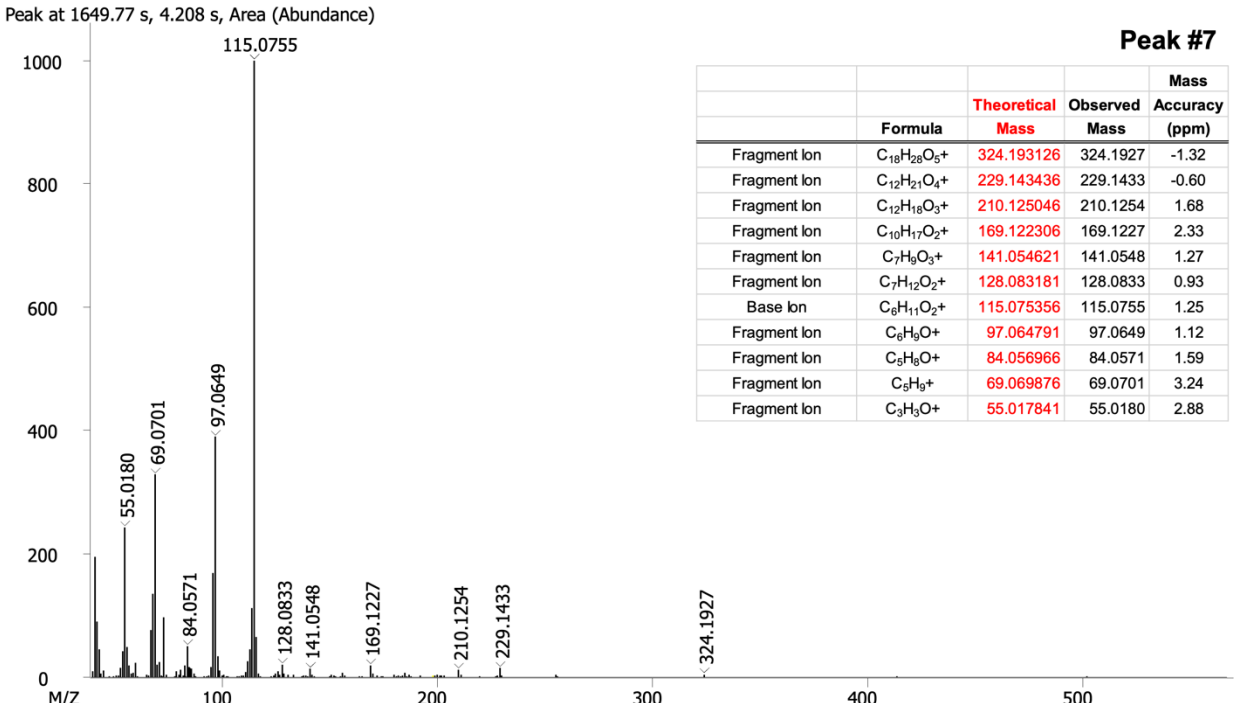

Peak #7

	Formula	Theoretical Mass	Observed Mass	Mass Accuracy (ppm)
Fragment Ion	$C_{18}H_{28}O_5$+	324.193126	324.1927	-1.32
Fragment Ion	$C_{12}H_{21}O_4$+	229.143436	229.1433	-0.60
Fragment Ion	$C_{12}H_{18}O_3$+	210.125046	210.1254	1.68
Fragment Ion	$C_{10}H_{17}O_2$+	169.122306	169.1227	2.33
Fragment Ion	$C_7H_9O_3$+	141.054621	141.0548	1.27
Fragment Ion	$C_7H_{12}O_2$+	128.083181	128.0833	0.93
Base Ion	$C_6H_{11}O_2$+	115.075356	115.0755	1.25
Fragment Ion	C_6H_9O+	97.064791	97.0649	1.12
Fragment Ion	C_5H_8O+	84.056966	84.0571	1.59
Fragment Ion	C_5H_9+	69.069876	69.0701	3.24
Fragment Ion	C_3H_3O+	55.017841	55.0180	2.88

Figure S30. Mass spectrum of peak 7. Refer to **Figure 4** for chromatographic positioning.

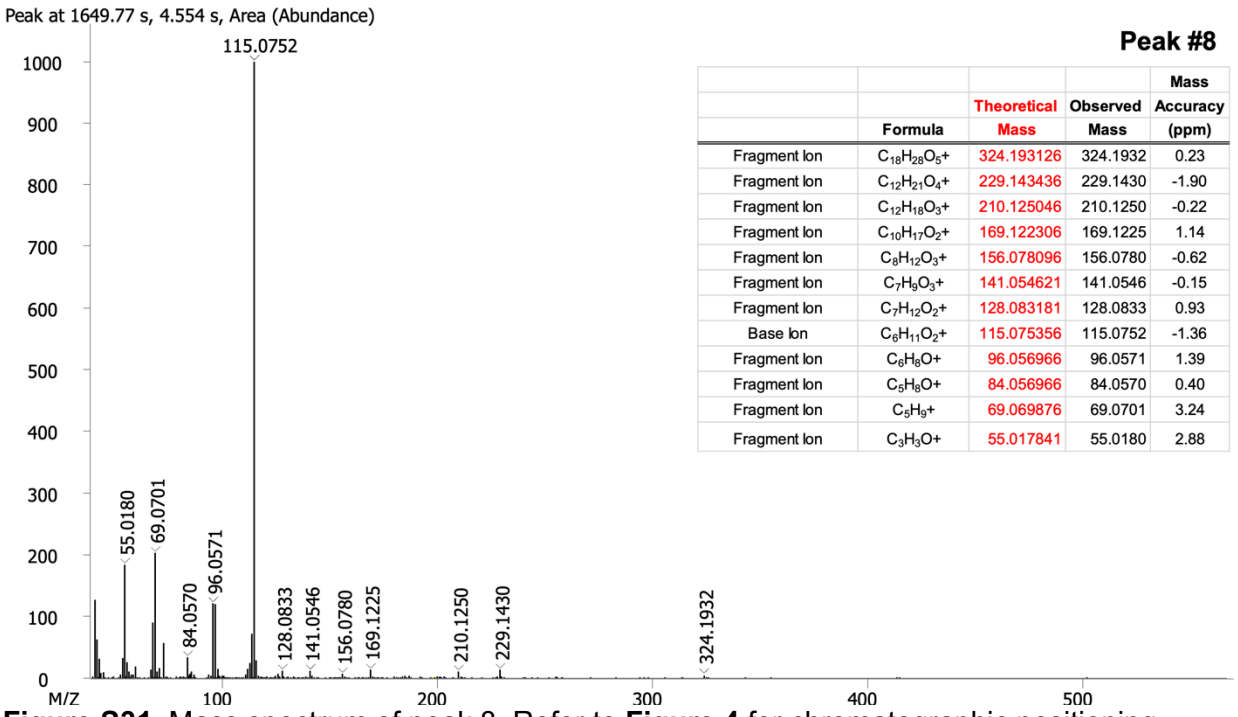

Peak #8

	Formula	Theoretical Mass	Observed Mass	Mass Accuracy (ppm)
Fragment Ion	$C_{18}H_{28}O_5$+	324.193126	324.1932	0.23
Fragment Ion	$C_{12}H_{21}O_4$+	229.143436	229.1430	-1.90
Fragment Ion	$C_{12}H_{18}O_3$+	210.125046	210.1250	-0.22
Fragment Ion	$C_{10}H_{17}O_2$+	169.122306	169.1225	1.14
Fragment Ion	$C_8H_{12}O_3$+	156.078096	156.0780	-0.62
Fragment Ion	$C_7H_9O_3$+	141.054621	141.0546	-0.15
Fragment Ion	$C_7H_{12}O_2$+	128.083181	128.0833	0.93
Base Ion	$C_6H_{11}O_2$+	115.075356	115.0752	-1.36
Fragment Ion	C_6H_8O+	96.056966	96.0571	1.39
Fragment Ion	C_5H_8O+	84.056966	84.0570	0.40
Fragment Ion	C_5H_9+	69.069876	69.0701	3.24
Fragment Ion	C_3H_3O+	55.017841	55.0180	2.88

Figure S31. Mass spectrum of peak 8. Refer to **Figure 4** for chromatographic positioning.

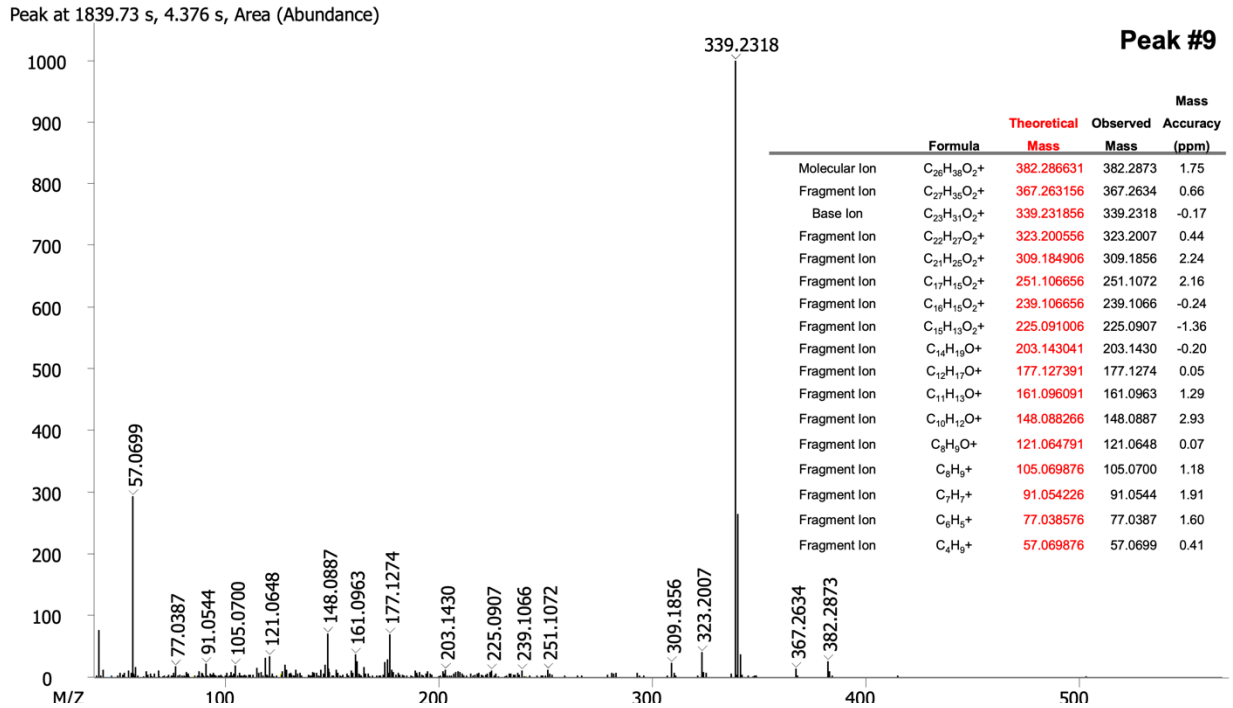

Peak #9

	Formula	Theoretical Mass	Observed Mass	Mass Accuracy (ppm)
Molecular Ion	$C_{26}H_{38}O_2$+	382.286631	382.2873	1.75
Fragment Ion	$C_{27}H_{35}O_2$+	367.263156	367.2634	0.66
Base Ion	$C_{23}H_{31}O_2$+	339.231856	339.2318	-0.17
Fragment Ion	$C_{22}H_{27}O_2$+	323.200556	323.2007	0.44
Fragment Ion	$C_{21}H_{25}O_2$+	309.184906	309.1856	2.24
Fragment Ion	$C_{17}H_{15}O_2$+	251.106656	251.1072	2.16
Fragment Ion	$C_{16}H_{15}O_2$+	239.106656	239.1066	-0.24
Fragment Ion	$C_{15}H_{13}O_2$+	225.091006	225.0907	-1.36
Fragment Ion	$C_{14}H_{19}O$+	203.143041	203.1430	-0.20
Fragment Ion	$C_{12}H_{17}O$+	177.127391	177.1274	0.05
Fragment Ion	$C_{11}H_{13}O$+	161.096091	161.0963	1.29
Fragment Ion	$C_{10}H_{12}O$+	148.088266	148.0887	2.93
Fragment Ion	C_8H_9O+	121.064791	121.0648	0.07
Fragment Ion	C_8H_9+	105.069876	105.0700	1.18
Fragment Ion	C_7H_7+	91.054226	91.0544	1.91
Fragment Ion	C_6H_5+	77.038576	77.0387	1.60
Fragment Ion	C_4H_9+	57.069876	57.0699	0.41

Figure S32. Mass spectrum of peak 9. Refer to **Figure 4** for chromatographic positioning.

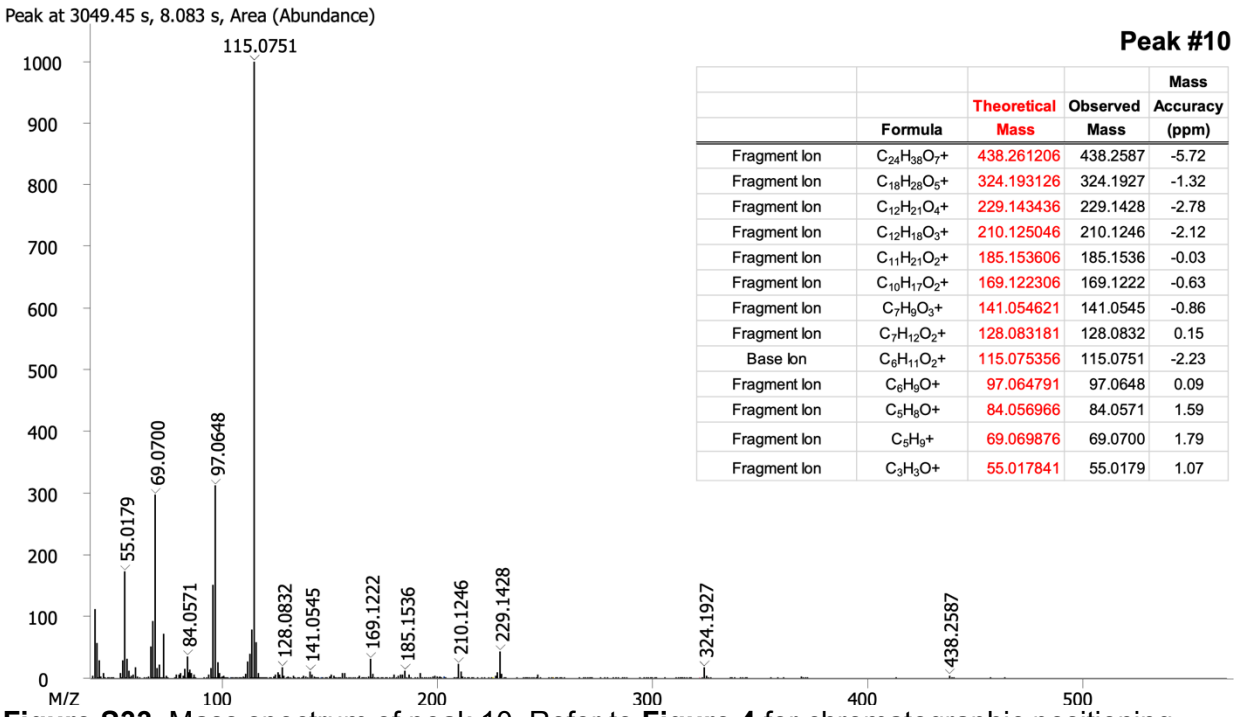

Peak #10

	Formula	Theoretical Mass	Observed Mass	Mass Accuracy (ppm)
Fragment Ion	$C_{24}H_{38}O_7$+	438.261206	438.2587	-5.72
Fragment Ion	$C_{18}H_{28}O_5$+	324.193126	324.1927	-1.32
Fragment Ion	$C_{12}H_{21}O_4$+	229.143436	229.1428	-2.78
Fragment Ion	$C_{12}H_{18}O_3$+	210.125046	210.1246	-2.12
Fragment Ion	$C_{11}H_{21}O_2$+	185.153606	185.1536	-0.03
Fragment Ion	$C_{10}H_{17}O_2$+	169.122306	169.1222	-0.63
Fragment Ion	$C_7H_9O_3$+	141.054621	141.0545	-0.86
Fragment Ion	$C_7H_{12}O_2$+	128.083181	128.0832	0.15
Base Ion	$C_6H_{11}O_2$+	115.075356	115.0751	-2.23
Fragment Ion	C_6H_9O+	97.064791	97.0648	0.09
Fragment Ion	C_5H_8O+	84.056966	84.0571	1.59
Fragment Ion	C_5H_9+	69.069876	69.0700	1.79
Fragment Ion	C_3H_3O+	55.017841	55.0179	1.07

Figure S33. Mass spectrum of peak 10. Refer to **Figure 4** for chromatographic positioning.

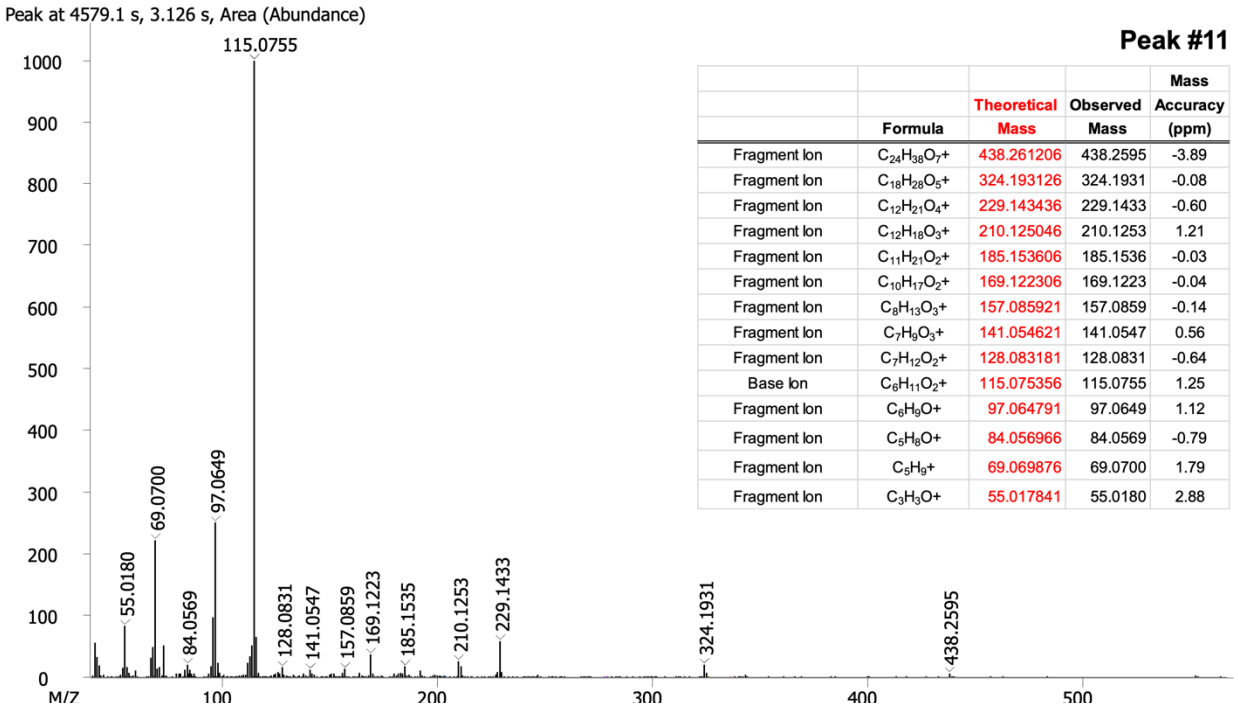

Peak #11

	Formula	Theoretical Mass	Observed Mass	Mass Accuracy (ppm)
Fragment Ion	$C_{24}H_{38}O_7$+	438.261206	438.2595	-3.89
Fragment Ion	$C_{18}H_{28}O_5$+	324.193126	324.1931	-0.08
Fragment Ion	$C_{12}H_{21}O_4$+	229.143436	229.1433	-0.60
Fragment Ion	$C_{12}H_{18}O_3$+	210.125046	210.1253	1.21
Fragment Ion	$C_{11}H_{21}O_2$+	185.153606	185.1536	-0.03
Fragment Ion	$C_{10}H_{17}O_2$+	169.122306	169.1223	-0.04
Fragment Ion	$C_8H_{13}O_3$+	157.085921	157.0859	-0.14
Fragment Ion	$C_7H_9O_3$+	141.054621	141.0547	0.56
Fragment Ion	$C_7H_{12}O_2$+	128.083181	128.0831	-0.64
Base Ion	$C_6H_{11}O_2$+	115.075356	115.0755	1.25
Fragment Ion	C_6H_9O+	97.064791	97.0649	1.12
Fragment Ion	C_5H_8O+	84.056966	84.0569	-0.79
Fragment Ion	C_5H_9+	69.069876	69.0700	1.79
Fragment Ion	C_3H_3O+	55.017841	55.0180	2.88

Figure S34. Mass spectrum of peak 11. Refer to **Figure 4** for chromatographic positioning.

REFERENCES

(1) Cowger, W.; Steinmetz, Z.; Gray, A.; Munno, K.; Lynch, J.; Hapich, H.; Primpke, S.; De Frond, H.; Rochman, C.; Herodotou, O. Microplastic Spectral Classification Needs an Open Source Community: Open Specy to the Rescue! *Anal Chem* **2021**, *93* (21), 7543–7548. https://doi.org/10.1021/acs.analchem.1c00123.